5 Determination of the real refractive index

5.1 Aim of study

The results obtained from the previous study showed the importance of the refractive index, to analyse results from laser diffractometry correctly. Unfortunately for most of the compounds no refractive index can be obtained from the literature. Therefore in this chapter possibilities for the determination of the refractive index were investigated. The real refractive index was obtained for some selected nanosuspensions and NLC formulations in order to investigate to which extent the refractive changes for the different systems. To investigate the usefulness of these parameters for LD measurements, the optical parameters obtained were applied in LD measurements and compared with the results from photon correlation spectroscopy and light microscopy.

5.2 Methods to determine the real refractive index

Literature screening gave view possibilities to determine the refractive index of solids and suspensions, which are nicely described in (Malvern 2004; Rawle 2004; Rawle 2006). The most appropriate methods where selected to be the observation of the Becke line and the determination of the differential refractive index. All other methods e.g. the determination by using polarisation microscopy or calculation via Gladestone Dale or Lorentz-Lorenz equation, were not carried out. Either due to a lack of the required instruments (polarisation microscope), other missing parameters (refractive indices of other polymorphs for Gladstone-Dale approximation) or as the results were estimated to be too inaccurate (immersion method, Lorentz-Lorenz equation).

5.2.1 Measurement of refractive index by analysis of dn/dc

The dn/dc, also called differential refractive index is the variation of the real refractive index due to a change in concentration of a solute. It is also known as the specific refractive index increment with the given symbol ν. It is expressed as g/ml. However, mostly it is called dn/dc.

$$\nu = \left.\frac{dn}{dc}\right|_{c=0} = \lim_{c\to 0}\left(\frac{n-n_0}{c}\right)$$

The measurement of dn/dc gives the possibility to calculate the unknown index of refraction of a compound. This is possible because the refractive index of a compound increases linearly with an increase in its concentration, when it is dissolved or diluted in another medium.

The procedure and the calculation of the refractive index is described in the literature (Huglin 1972; Wu and Xia 1994; Russo 2005). The procedure used was kindly adapted from the workgroup of R. Sigel (Sigel).

Different dilutions with various concentrations are prepared from the compound with the unknown refractive index. Afterwards the real index of refraction is measured for each solution prepared. Also a sample of pure dilution medium must be analysed. From the data obtained the differential index of refraction can be analysed. For that the measured index of the pure dissolution medium is subtracted from each index measured for the different concentrations. The obtained set of data is plotted in a diagram; where the concentration is plotted on the abscissa and the measured refractive index is plotted on the ordinate. From this the linear regression function can be calculated. The slope m of the function corresponds to the dn/dc in g/ml. In order to calculate the real refractive index of the unknown compound, the obtained differential refractive index is multiplied by 100 and the refractive index of the pure dissolution medium is added. The result corresponds to the real refractive index of the compound. It is important to mention that the concentrations need to be measured in w/v% as the differential refractive index is expressed in g/ml. However if the samples are weighted in as volumetric concentration (v/v%), the value obtained needs to be corrected. For this the obtained value for dn/dc has simply to be divided by the density of the compound with the unknown refractive index. The advantage of the dn/dc determination method is that any method for the measurement of the refractive index can be used (e.g. Abbe refractometer, interferometer) and various parameters can be considered (different wavelengths and various temperatures).

If particulate systems are analysed the concentration must be kept low, to avoid scattering effects from particles. The particle size should be small for the same reason, as well as to avoid sedimentation of particles during analysis. The determination coefficient of the regression should be at least 0.99 or higher, as the result is very sensitive to errors, leading to great variations in the calculated refractive index.

However, most of the systems analysed were not only suspended in water but also in surfactant or glycerol/water mixtures or even in unknown suspension media (e.g. latex suspensions). If the suspension medium is different to water, the pure dispersion medium needs to be analysed as the reference. Otherwise the calculated index of refraction will be incorrect. For instance a drug nanosuspension contains 1% of drug and is suspended in a 1% surfactant solution. When the sample is diluted with water 1:1 also the concentration of the surfactant is diluted 1:1. If no correction is considered the result would be a combination of

the refractive index of the particles and the surfactant. In Figure 5-1 an example is given for the cyclosporine nanosuspension. Determination and dilution with water yields a refractive index of 1.484, whereas the index is higher (1.497) when measured in the distinct stabiliser solution, i.e. Poloxamer 188 0.5% in water.

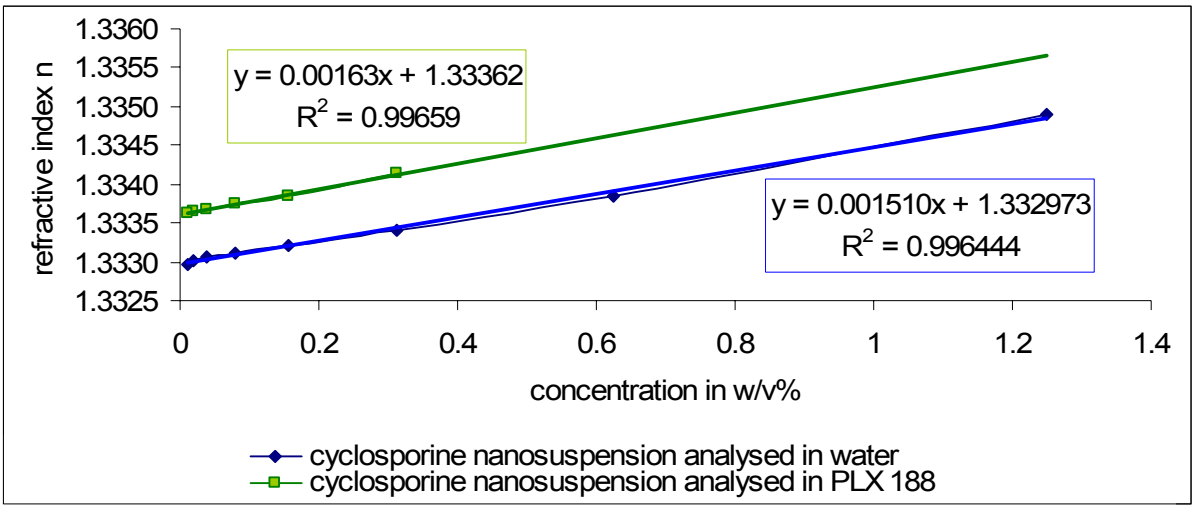

Figure 5-1: dn/dc for cyclosporine nanosuspension (NS) determined in water and PLX 188 solution

Therefore those samples must be measured and diluted with the original suspension medium, which can be prepared if the composition is known. If not, the procedure is more time consuming, as particles need to be separated from the medium, to obtain pure dispersion medium. In this study all dispersion media of the nanosuspensions and latex particles were obtained by the separation of particles form the dispersion medium.

The dn/dc was determined using the Abbemat which determines the refractive index by analyisis of the critical angle of total reflection. For the cylsosporine, ADA and carbamazepine nanosuspensions the refractive index could also be analysed by using a scan ref, which is based on interferrometry measurements.

Table 5-1 – Table 5-10 show the compositions of the systems analysed. The rational behind selecting these particles was to have one group with identical stabiliser (lecithin) but differing in the composition of the particle matrix (LCT; MCT: LCT mixture 50:50 and a wax). In a second group the particles matrix is identical, but the stabiliser is different. In the next group the incorporated drug was different. To change certain parameters of the particles should allow assessing each specific contribution to the real refractive index.

Table 5-1: Fat emulsions and SLN - identical in stabiliser and dispersion medium

1		2		3	
Lipofundin N 10%		Lipofundin MCT 10%		formulation C6 LC lipid (=SLN)	
compound	w%	compound	w%	compound	w%
soy bean oil (=LCT)	10.0	soy bean oil (=LCT)	5.0	cetylpalmitate (=wax)	10.0
egg lecithin	0.8	egg lecithin	0.8	egg lecithin	0.8
glycerol	2.5	glycerol	2.5	glycerol	2.5
		medium chain triglycerides (=MCT)	5.0		

Table 5-2: Cetylpalmitate NLC - identical in lipid composition, different in stabiliser or incorporated drug

4		5		6		7	
batch code: Stab. 1 with vitamin E		batch code: Stab. 1		batch code: Stab. 2		batch code: Stab. 3	
compound	w%	compound	w%	compound	w%	compound	w%
cetylpalmitate	12.0	cetylpalmitate	15.0	cetylpalmitate	15.0	cetylpalmitate	15.0
Miglyol 812	4.0	Miglyol 812	5.0	Miglyol 812	5.0	Miglyol 812	5.0
Tegocare 450	1.8	Tegocare 450	1.8	Poloxamer 188	1.8	Tween 80	1.8
α-Tocopherol	4.0						

Table 5-3: Softisan SLN - identical in lipid composition – different in incorporated drug

8		9	
batch code: Softisan SLN placebo		batch code: Softisan SLN with liponic acid	
compound	w%	compound	w%
Softisan 601	10.0	Softisan 601	9.5
Miranol Ultra C32	1.2	Miranol Ultra C32	1.2
		liponic acid	0.5

Table 5-4: Stearyl alcohol NLC - identical in lipid composition – different in incorporated drug

10		11		12	
batch code: stearly alcohol NLC /sunflower oil		batch code: stearly alcohol NLC placebo		batch code: stearly alcohol NLC with tretinoine	
compound	w%	compound	w%	compound	w%
stearyl alcohol	10.5	stearyl alcohol	18.0	stearyl alcohol	17.73
sun flower oil	4.5	Miglyol 812	2.0	Miglyol 812	1.97
Tween 80	3.0	Tween 80	2.0	Tween 80	2.0
				tretinoine	0.3

Table 5-5: Dynasan NLC

13	
batch code: Dynasan	
compound	w%
Dynasan 116	20.0
Tyloxapol	5.0

Table 5-6: Nanosuspensions – different in drug – similar in stabiliser (Tween 80)

14		15		16		17	
ADA (30.4.04 cycle 20 0°C RT ASLI)		budesonide (20.5.03 cycle 20 0°C RT ASLI)		carbamazepine (17.4.03 cycle 20 45°C RT ASLI)		itraconazole (28.1.03 cycle 20 10°C RT ASLI)	
compound	w%	compound	w%	compound	w%	compound	w%
azodicarbonamide (ADA)	1.0	budesonide	1.0	carbamazepine	1.0	itraconazole	1.0
Tween 80	0.5	Tween 80	0.5	Tween 80	0.5	Tween 80	0.5

Table 5-7: Nanosuspensions – different in drug – similar in stabiliser (PLX 188)

18		19		20		21	
bethamethason-valerat (BMV 01 25.8.04 Cycle 20 RT)		budesonide (BCH Z-40))		cyclosporine (C3-Spüli 5.3.04 KS)		buparvaqoune (xxx)	
compound	w%	compound	w%	compound	w%	compound	w%
bethamethason-valerat	1.0	budesonide	1.0	cyclosporine	0.53	buparvaquone	1.0
PLX 188	1.0	PLX 188	1.0	PLX 188	0.25	PLX 188	0.5
		Chitosan chloride	0.5				

Table 5-8: Latex dispersions

22		23		24	
BMG 32		60/II		SCA18	
compound	w%	compound	w%	compound	w%
polysterene latex	7.2	polysterene latex	4.45	polysterene latex	4.7
PEG		PEG		PEG 200	

Table 5-9: Nanosuspensions analysed with scan ref

25		26		20	
cyclosporine (C3-Spüli 5.3.04 KS)		carbamazepine (C4 Carb1 oG-KS)		azodicarbonamide (ADA) (C3-ADA 20n)	
compound	w%	compound	w%	compound	w%
cyclosporine	0.53	carbamazepine	1.0	azodicarbonamide	1.0
PLX 188	0.25	PLX 188	0.5	PLX 188	0.5

Table 5-10. Various other compounds analysed

Surfactants:	SDS	PLX 188	Tween 80
Oils:	linseed oil	miranol ultra	Miglyol 812
almond oil	peanut oil	peppermint oil	olive oil
sun flower oil	poppy seed oil	soy bean oil	corn oil
saflor oil	castor oil	fish oil	

5.2.1.1 Determined indices for selected lipid systems and nanosuspensions

Table 5-11: Real refractive indices for various systems analysed with Abbemat

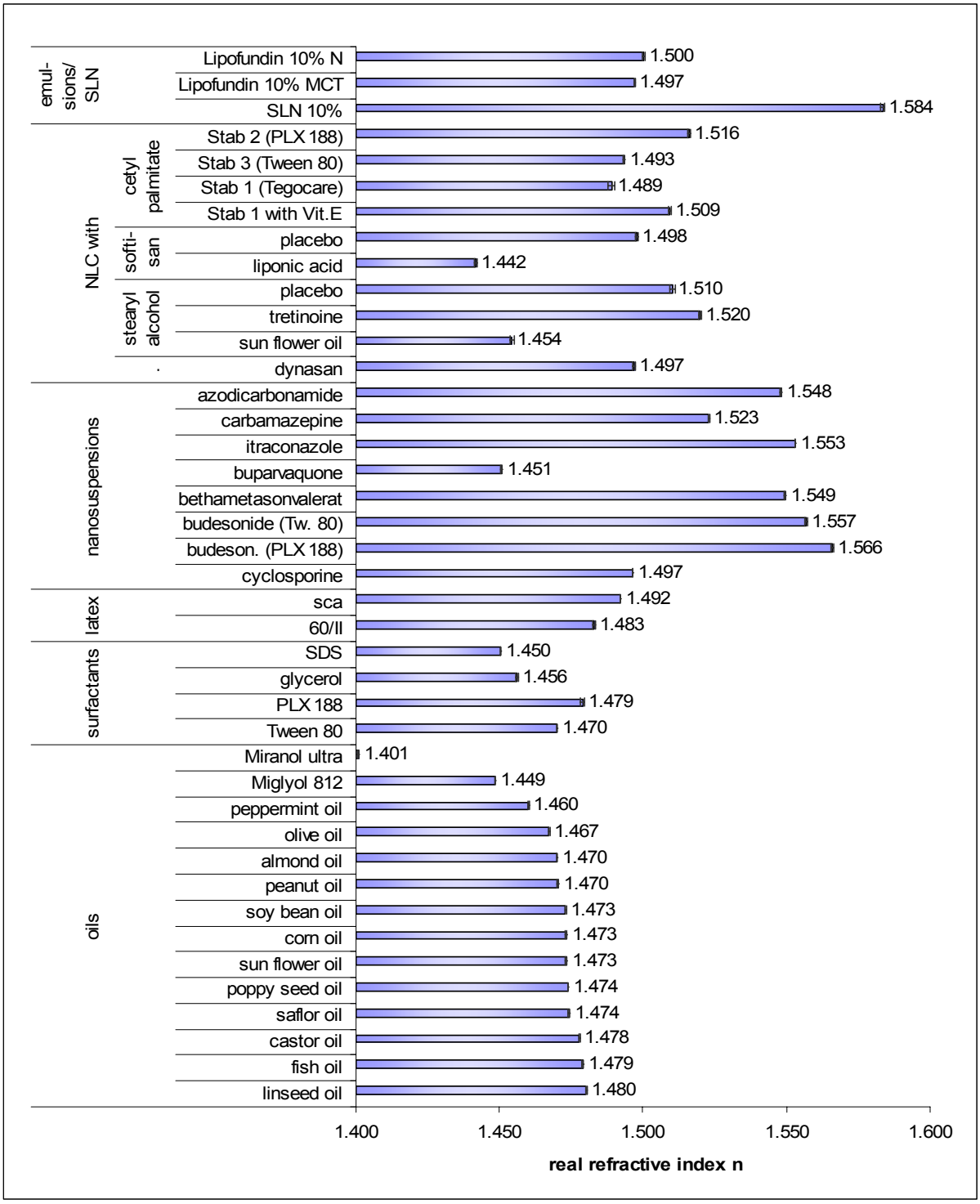

The results show, that the indices are different for each system analysed. It was not only dependent on the main component, e.g. oil or drug, but also on the stabiliser used. Critically it needs to mentioned that the concentrations used for the determination were not controlled by an extra method e.g. HPLC (except for cyclosporine nanosuspension). It was assumed that the concentrations remained constant over the whole homogenisation process when preparing the

dispersions. As this cannot be guaranteed the values obtained most likely are not the absolute indices. However from the small standard deviations it can be seen that the method itself is highly suitable for the determination of the real refractive index.

5.2.1.2 Limitations of the method

For the system Latex BMG 22 irregular and negative refractive indices were obtained, resulting in a refractive index smaller than water (Figure 5-2) As this is not logical the obtained result was checked by using a different method to obtain information about the refractive index (see 5.2.2)

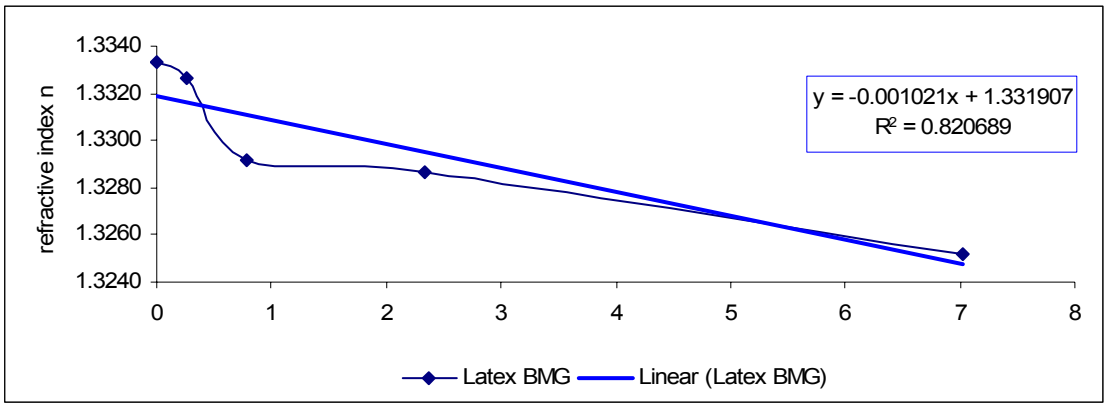

Figure 5-2: Determined dn/dc for Latex BMG 22, would give a real refractive of 1.2298 which is smaller than the refractive index of water – the result is not correct

5.2.2 Analysis of real refractive index by observation of the Becke line

The Becke line method is usually utilised to determine if the crystal or the particle of question has a lower or higher index of refraction than the surrounding medium. The Becke line is a band or a rim of light visible along a particle or crystal boundary in light.

A Becke line is the result of two facts. Both are related to refraction along the boundaries of particles. First there is the fact that particles act as lenses as they tend to be thicker in the centre and thinner towards the edges. Therefore, if the real index of refraction is higher as the surrounding medium, the rays of the incident light converge towards the centre of the particle. If the index of refraction is lower than the surrounding medium the rays converge towards the edge of the particle. Internal reflection of the incident light occurs within the particle due to the presence of vertical particle boundaries. These two effects concentrate the light into a thin band within an object with a high index of refraction (1997)(1997)(1997)(Schmidt and Heidermanns 1958; El-Hinnawi 1966; Richardson 1991; Stroiber and Morse 1994; 1997; Derochette 2005).

In the previous chapter Latex BMG 22 was analysed by measuring dn/dc using an Abbemat refractometer. The analysed results of the dn/dc measurement indicated a real index of

refraction smaller than water. The result is unexpected and there was a need to prove the result obtained from this analysis. The investigation of the Becke line is time consuming, but the advantage is a visible and therefore a doubt free result.

For the experiment the latex dispersion was diluted with water (1:50). The Becke line of the dispersion was observed by light microscopy at higher and lower positions. In order to compare the results to a standard, the Becke line was also investigated for air bubbles (lower refractive index than water) and for dust particles (higher refractive index than water). The images obtained are shown in Figure 5-3 for the standards and in Figure 5-4 for the Latex dispersion.

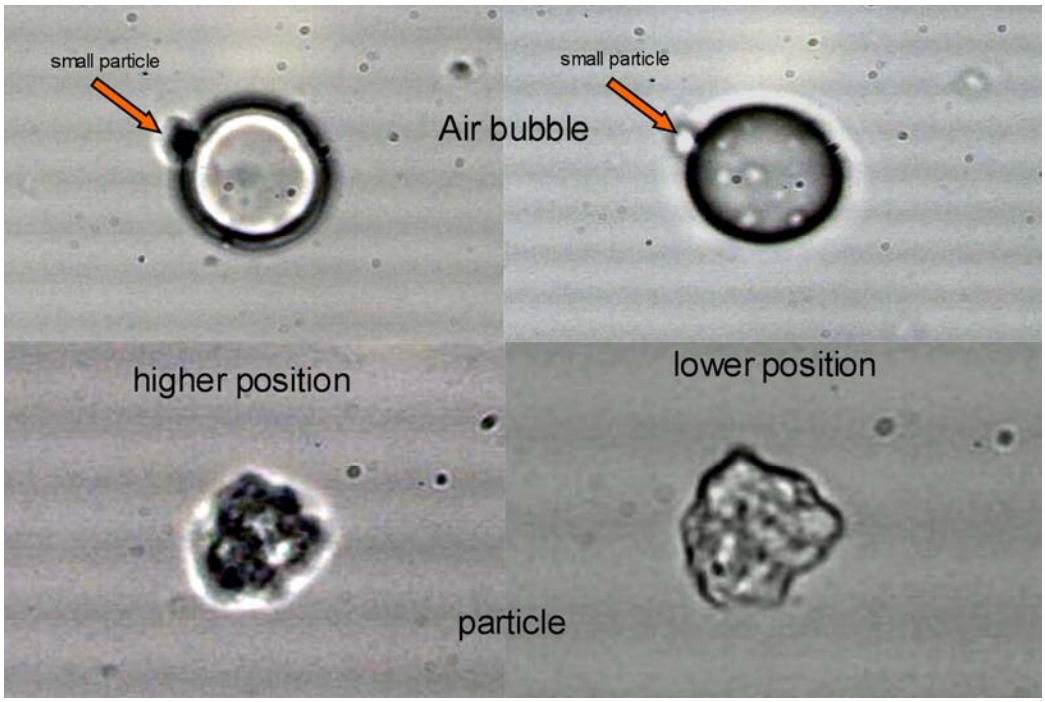

Figure 5-3: Becke line of air bubbles and a small particle (attached to air bubble) in water (upper) and for dust particles (lower) at higher (left) and lower (right) positions under the microscope.

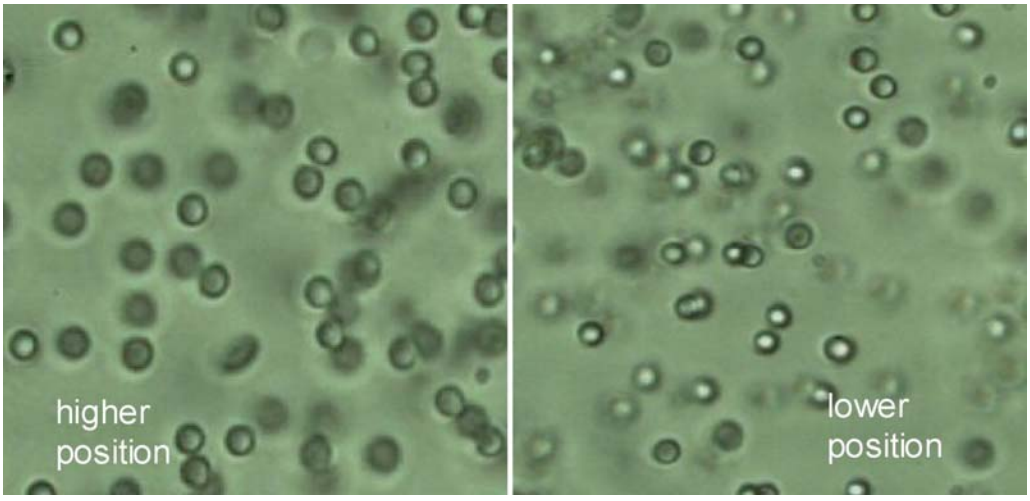

Figure 5-4: Becke line of latex particles, effects are the same as for dust particles

Air bubbles have a smaller index of refraction than water. Air bubbles are illuminated inside at upper positions. If the position is lowered the objects becomes dark and a bright ring around the object occurs. It is the opposite case if the object has a higher index of refraction than the surrounding medium. This can be as seen for the dust particles and the small particles next to the air bubbles.

When the latex dispersion was analysed, no effects were observed during microscopy, as the particles were too small for the observation of the Becke line. However, the enlargement of the images taken during microscopy analysis by computer led to a clearly visible result. The latex particles are dark and surrounded by a bright line at higher positions. When the position is lowered the particles become illuminated inside, which is similar to the dust particles. From this it is concluded, that latex BMG has a higher index of refraction than water. It also gives evidence that the results obtained from the previous analyses included an error. It is assumed that the reason of the error observed is the particle size of the latex particles. The principle of the Abbemat refractometer is the measurement of the critical angle, where total reflection occurs. Therefore light intensity is measured under different angles. The angle where a minimum of measured light intensity is observed corresponds to the critical angle. The particle size of the latex dispersion BMG 22 is 1.7µm which is about 3 times higher than the wave length used for the dn/dc measurement (632.8nm). With this ratio of particle size to wavelength, the BMG 22 latex particles show Fraunhofer scattering characteristics. Fraunhofer scattering is characterised by an intense forward scattering, but weak back scattering, which means that the scattered intensity strongly depends on the angle of incident light. Thus the scattering effects from the particles my disturb a correct detection of the critical angle, as the minimum of light due to total reflection is overwhelmed by scattered light.

5.2.3 Measurement of refractive index with manual Abbe refractometer

Also the Abbe refractometer measures the index of refraction by the measurement of the critical angle of total reflection. In contrast to the digital Abbemat refractometer, the bright/dark field boarder is observed visually. Therefore, if disturbance due to light scattering occurs it is expected to see an unsharp and fuzzy boarder line or even no boarder.

The samples listed in Table 5-12 were analysed using a manual ABBE refractometer (Carl Zeiss, Jena). Table 5-12 also gives the result of the observations from the experiment. All NLC/SLN systems gave a sharp line between the bright and the dark field. Latex particles 60II and SCA also gave a clear sharp line. When nanosuspensions were observed the line was

Table 5-12: Analysed samples and results of analysis

NLC/SLN	Stab 1	sharp line visible
	Vit E	sharp line visible
	Stab 2	sharp line visible
	Stab 3	sharp line visible
	CL Lipid	sharp line visible
	Dynasan	sharp line visible
latex	sca18	sharp line visible
	60II	sharp line visible
	BMG 22	**no line**
nanocrystals	budesonide	sharp line visible, some fuzziness
	itraconazole	sharp line visible, some fuzziness
	carbamazepine	sharp line visible, some fuzziness
	ADA	sharp line visible, some fuzziness
	cyclosporine	sharp line visible, some fuzziness

existent, but some fuzziness was visible. No line was visible when latex particles BMG 22 were analysed. In order to correlate the results from Table 5-12 with the size all samples were analysed by PCS and laser diffractometry. UV/Vis spectroscopy was also performed. UV/Vis spectroscopy is mainly used to measure the absorption of compounds dissolved in a liquid. From the determined absorption the concentration can be calculated according to Lambert Beer`s law. If particular systems are analysed possible scattering phenomena from the particles need to be considered. According to the scattering phenomena of particles (see 4.1), particles larger than the wavelength will have stronger forward scattering than particles smaller than the wavelength. Differences in the detected intensities are also expected if a particle dispersion (constant size and concentration) is analysed with different wavelengths. If one decreases the ratio between the particle size and the wavelength the forward scattering of the particle increases. This leads to a higher intensity on the detector (determined as transmission) and a smaller absorption therefore. The rational behind the UV/Vis measurements of this study was to gain information about possible differences in the wave length dependent scattering of the particles. It was hoped to see wavelength dependent increases or decreases for the different particles and particle sizes. The dilution of the particle dispersions in the same manner seemed to be difficult, because all dispersions were different in particle size and particle concentration. On order to obtain a standard, the concentration of the particle dispersions was adjusted using the laser diffractometer LS 230. This is possible as the instrument measures the obscuration of the sample in the PIDS cell prior the measurement. The obscuration in principle is the measurement of the transmission, which means all samples were diluted in order to obtain the same transmission at 450nm (= PIDS obscuration). The samples were obtained by preparing the LS 230 for a measurement with included PIDS. After alignment, background measurement and the de-bubbling procedure

each sample was added to the sample cell until a PIDS obscuration of 45% was reached. The cell was flushed and the diluted sample collected and analysed by UV/Vis spectroscopy immediately. Figure 5-5 and Figure 5-6 show the data obtained from the measurements.

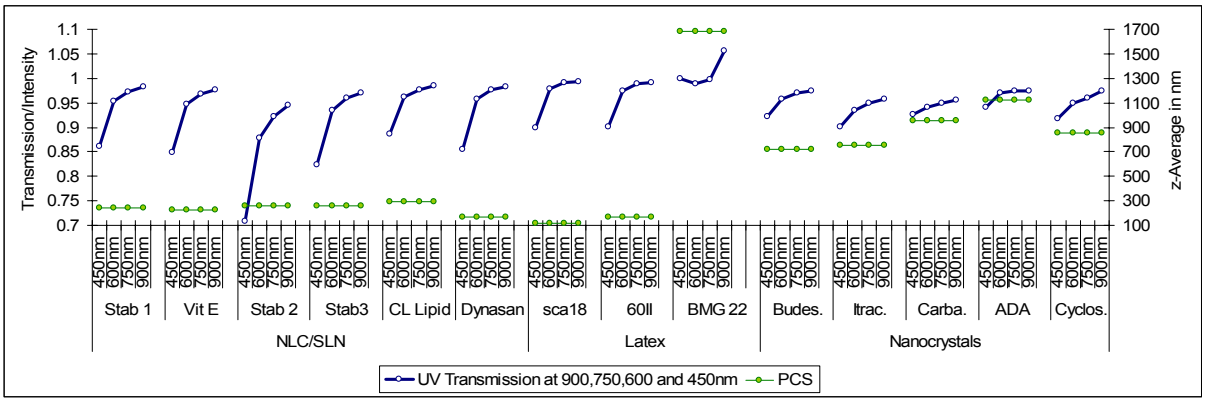

Figure 5-5: UV/Vis Transmission for 450, 600, 750 and 900nm and PCS values for the systems

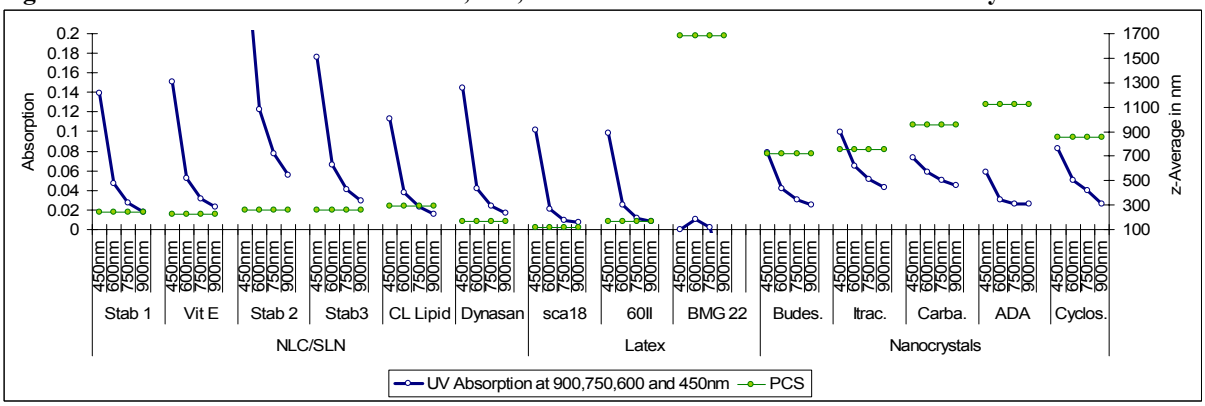

Figure 5-6: UV/Vis Absorption for 450, 600, 750 and 900nm and PCS values for the systems

In all systems the transmission increased, when the wave length was increased. Only latex (BMG 22) showed a trend different to the systems. Here the transmission decreased when the wave length was increased, as it was expected to see.

In conclusion, two effects lead to the absorption and transmission values measured. If particles are present in the sample analysed, they interfere with the light beam of the instrument in a size dependent manner. If particles are small and the wavelength is large, the interference is small. If particles are about the same size than the wavelength or larger, the interference is larger too. If the size is kept constant and the wavelength is increased, the interference of light with the particles decreases with an increase of wavelength. This effect was seen for all samples, expect for Latex dispersion BMG 22. Here the second and expected effect could be observed. If light co-interacts with a particle scattering effects occur (e.g. diffraction, refraction, reflection). Also here the effects are size dependent. The larger the particle size in comparison to the incident wavelength, the more intense is the forward scattered light intensity. This means with an increase in particle size the detected light

intensity from forward scattered light increases in a wavelength dependent manner. At a certain particle size the intensity from scattering overwhelms the effect of absorption and interference measured for smaller particles. In case of the latex particles the absorption value measured for 450nm was even negative, clearly indicating a higher intensity on the detector than in the medium without particles which derived from scattering of the particles.

From this it is concluded, that the refractive index of particles much larger than the wavelength of the refractometer used can not be analysed due to scattering effects, which disturb the detection of the total reflection, if disturbance occurs can be investigated by using a manual Abbe refractometer. If the line between dark and broad field is sharp, the sample can be analysed. UV/Vis spectroscopy also gives information about scattering effects. If a sample can be analysed, the absorption values of the sample measured must decrease with an increase in wavelength. If the trend is an increase of absorption with an increase in wavelength scattering effects from particles are too intense and overwhelm other effects, e.g. refraction, making an analysis impossible. Therefore particles to be analysed should be as small as possible to keep the effect of scattering low.

The investigation of the Becke line is possible. Only particles larger 1µm can be analysed, as the enlargement of the light microscope is limited. This method only gives a rough result of the refractive index. The advantage is the visible and doubt free result therefore. Of course to approach the real refractive index dispersion media for the particles need to be used having different refractive indices. By determining whether the refractive index of the representative liquid is higher or lower, one can stepwise approach the particle index.

5.2.4 Real refractive index obtained from interferometry

In Figure 5-7 the indices which were obtained from the measurement with the Abbemat and the scan ref are compared.

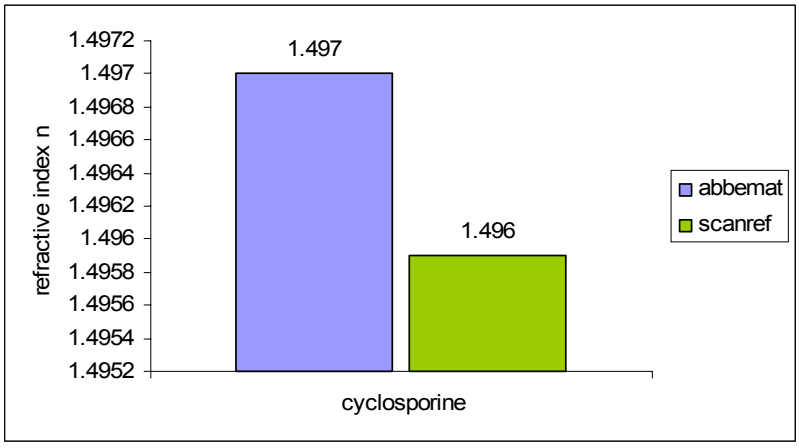

Figure 5-7: Real refractive indices obtained for cyclosporine nanosuspension with scan ref (green) and Abbemat (blue)

The results are almost the same and differ only in the third digit after the dot. However the index of refraction is dependent on the temperature and the wavelength and decreases if both are increased. The Abbemat analyses the refractive index at the sodium wavelength (589.3nm) whereas the scan ref is operated at a wavelength of 632.8nm. Therefore the difference can be explained by the different wavelengths applied. In addition, for the particle size analysis it needs to be considered that the LS 230 operates with a laser having a wavelength of 750nm. Hence the index of refraction measured at a lower wavelength is higher if the sample is analysed in the LS 230. Moreover it was found that the temperature, at which the measurement takes place in the LS 230, is not - as probably assumed - 20°C but higher up to 31°C. Therefore the refractive index further decreases.

5.2.5 Changes of the real index of refraction due to hydration

Within the study also liquid polyethylene glycols (PEGs) have been analysed, by determining dn/dc, primarily to prove the accuracy of the method. However the refractive indices which were obtained from dn/dc calculations were not in agreement with the indices obtained from the pure liquids and from the data found in the literature. All indices analysed were smaller as expected (Figure 5-8).

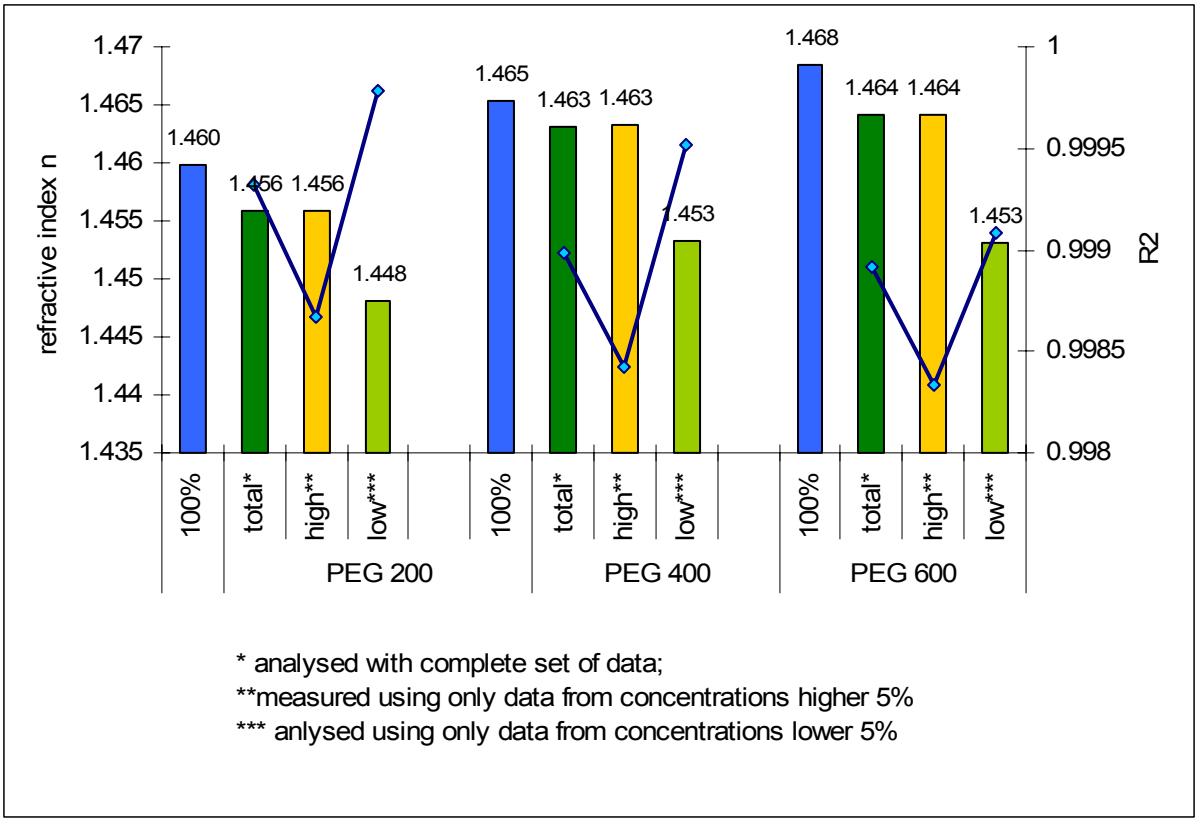

Figure 5-8: Refractive indices for various polyethylene glycols obtained from pure liquid (= 100%) and determined from dn/dc measurements

The observation can be explained by the fact that PEGs show strong hydration phenomena when dissolved in water, which can be observed by measuring the changes in temperature. For the experiment 50.00g PEG were weighted in into a 100ml volumetric flask and filled up with water. The temperature was determined at its highest point using a digital thermometer (IKA-TRON DTM 10, Janke and Kunkel, Staufen, Germany). The following dilutions (25%, 12.5%, 6.25%, and 3.125%) were obtained by placing 50.0ml of the previous dilution into a 100ml volumetric flask and filling up the flask with water. The temperatures were measured as described above. The data obtained are shown in Figure 5-9. The temperature increases if water is added to the PEGs. With ongoing dilution the changes in temperatures decrease. At a concentration of 3.125 %, no differences can be measured anymore when more water is added. Therefore this concentration was thought to be related to the complete hydration of the PEGs.

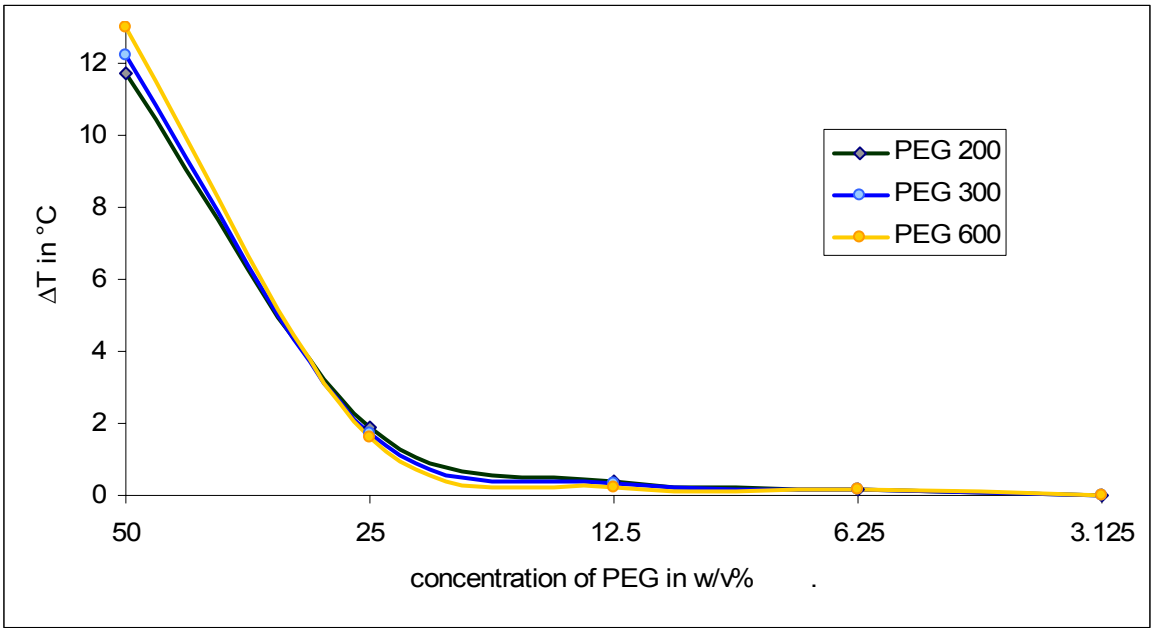

Figure 5-9: Increase in temperature due to hydration of the PEGs

From this the data of dn/dc measurements were analysed by only calculating the refractive index from the data of higher concentrations (>5%) and lower concentrations (< 5%), from the latter it was assumed that PEGs were fully hydrated (Figure 5-8, orange and light green columns). By comparing the determination coefficients (R^2), it was found that it was higher when fully hydrated PEGs (low concentrations) were analysed, but it was low when only partly PEGs (higher concentrations) were analysed. Which means only low concentrations, were no changes in temperature were observed, yielded accurate and therefore correct results in principle, whereas concentrations were the temperature was still increasing upon the addition of water, give non-linear results. The refractive indices obtained from low

concentrations are much smaller than those from the pure liquids. In conclusion: hydration of PEGs decreases the real refractive index. The decrease due to hydration was about 0.015 in total. Even if the difference seems little, it should be considered.

5.2.6 Time dependent changes in refractive index

The dn/dc of a cyclosporine nanosuspension was analysed at different times after the production. The results which are shown in Figure 5-10 indicate that the refractive index increases over the time of storage. Any loss of dilution medium due to evaporation could be excluded by the determination of the total concentration of cyclosporine via HPLC. Therefore it is assumed that the index changes due to a change in the crystalline state of the nanocrystals (e.g. transformation from amorphous to crystalline).

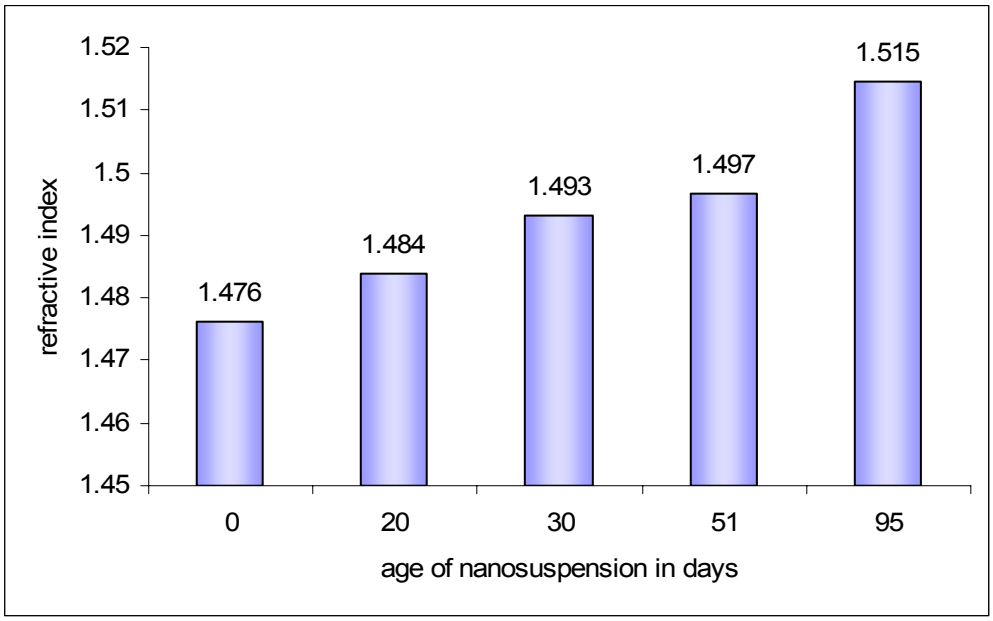

Figure 5-10: Changes in refractive index of cyclosporine nanosuspension over time

5.2.7 Conclusion

In this study a method to determine the unknown refractive index for nanosuspensions and NLCs was established. The method determines the refractive index by the measurement of the specific refractive increment (dn/dc). It was shown, that the index of refraction is dependent on the main compound but also on the stabiliser or co-compounds. The method is not suitable for larger particles, as scattering caused by the interference disturbs the correct function of the instrument. The observation of the Becke line can be used to check doubtful results, but is not reliable for the detailed determination of the refractive index. Also a manual Abbe refractometer is not the appropriate instrument, as the resolution is only 0.002, which is too inaccurate for the determination of dn/dc, where mostly low concentration with little differences in RI are measured. However the Abbe refractometer was found to be useful if the

all over possibility for the determination of dn/dc needs to be checked. Only particles giving a sharp border can be analysed. Any fuzziness or no border indicates that particles are too large for analysis.

The refractive index is also influenced by the hydration effect, as studied for PEGs in this study. Hydrations were found to decrease the refractive index. More interestingly it was found that the refractive index of a cyclosporine nanosuspension increased over the time of storage. This observation should be investigated in more detail, as it may open a new perspective to observe changes in the crystalline state, which is up to now only possible by less convenient x-ray diffraction. Refractive index measurements might even be able to detect structural changes in the surface layer of nanoparticles which are not accessible by x-ray due to the resolution limit (5% of a fraction must be present in the sample to be detected).

In summary refractive indices can be analysed. However, as the refractive index strongly depends on the temperature and the wavelength, it would be more accurate to obtain the required refractive index at a wavelength similar to the one used for LD measurements. In the case of the LS 230 this is not possible, as no instrument operated at this wavelength is available on the market. Also further investigations should be carried out at temperatures similar to the temperature of the actual measurement. This was not taken into account here, as the measurements were conducted before the unexpected increased temperatures within LD measurements were realised.

5.3 Comparison of LD results obtained from measurements with and without correct optical parameters

In order to compare the meaning of correct optical parameters in practice, the systems from which the real refractive index was determined were analysed by laser diffractometry. For comparison the raw data were calculated using Fraunhofer approximation and Mie modus, where the standard value of 1.456 (Müller 1996) was compared to the definite determined values. Values for the imaginary indices were analysed as suggested by Beckman Coulter by simply determining UV/VIS absorption of the original sample in the dispersion medium. In addition all systems were characterised using PCS and light microscopy. In the following tables all data for each system are put together.

In Table 5-13 the data obtained for the Lipofundin MCT emulsion are shown. Microscopic imaging detected some droplets larger than 2µm, which were not found within LD measurements, neither by Fraunhofer approximation nor by both Mie calculations. The simulation gives particle sizes larger than 1µm only for high IRI values. The graph shown in the third row of the table shows the particle size distribution calculated. In this Fraunhofer detects a very small particle population of approximately 50nm, indicating the poor sensitivity of the calculation mode. Nevertheless small fractions of about 80nm were detected for both of the Mie calculations. If this peak is correct is hardly to decide, but might be alright as it is known, that unbound lecithin can form liposomes, being in this size. All over in this analysis the differences between the Mie calculations are neglectable small, whereas Fraunhofer approximation failed.

In Table 5-14 the data from the Lipofundin N 10% emulsion are shown. From microscopy no larger droplets were obtained, matching with the results from laser diffractometry therefore. Again Fraunhofer approximation failed, as the small peak already seen in the MCT emulsion also oocurs here. In contrast to the MCT formulation, Mie with the standard refractive index detected a smaller peak, thought to correspond to liposomes, whereas the refractive index determined did not detect the second particle population. Also here it is hard to decide which mode matches the real result best. The result only shows that a change of the refractive index changes the particle size and the size distribution. Depending on which mode used the interpretation of the results will vary, e.g. if the determined index is used the MCT emulsion would be thought to be more instable, as liposomes (second peak) were detected in comparison to the N formulation were no liposomes could be observed. In contrast; Mie mode with the standard value gives a second peak for both of the emulsion - here a differentiation is actually not possible. However, Fraunhofer gave incorrect results for both of the systems.

The data obtained for Stab 1 (NLC containing cetylpalimate, Miglyol 812 and Tegocare) are shown in Table 5-15. The analysis led to the same result. Fraunhofer gave a totally different size and size distribution as the Mie calculations, which were almost the same. However the simulation showed that the use of higher imaginary values (i.e. 1.0!) increases the particle size detected. In the distribution graph (third row) it is analysed as a third particle population at about 2µm, which was also seen from microscopy. However such high values are not correct. Therefore the matching result of that optical parameter with microscopy probably just occurred by chance. The lack of the detection of larger particles is thought to be related to the fact as already demonstrated. Larger particles are often not detected if PIDS is included into the measurement.

In contrast was Stab 2 (NLC as Stab 1 but stabilised with Poloxamer 188) (Table 5-16). As seen from microscopy the system consisted of large agglomerates and fat particles, whereas only a few nanoparticles were left. Large particles were detected in every calculation mode applied. However, Fraunhofer in this case failed to detect smaller particles. When Mie modus with optical parameters from (Müller 1996) was used the second peak at approx. 2µm is not found. Larger particles than 500µm are not detected in this modus, but in the Mie mode with correct optical parameters. All over, all analyses give the result of the existence of larger particles, but the Mie analysis with the determined index is best, as it resolves small particles, as well as it detects larger particles.

The data of Stab 3 (NLC as Stab1 and 2 but stabilised with Tween 80) (Table 5-17) also showed large particles in microscopy as well as in all LD calculations. The differences of the Mie calculations are little.

Fraunhofer analysis for the SLN stabilised with lecithin (Table 5-18) detected particles up to 3.206µm not found in images from microscopy. Also particles smaller than 60nm were detected incorrectly. Mie analysis after (Müller 1996) finds particles up to 869nm, whereas the analysis with the correct index of refraction detect particles up to 1.047µm, which were also seen from microscopy. The tendency is that Mie analysis after (Müller 1996) leads preferentially to too small particle sizes.

For the Dynasan NLCs, which are shown in Table 5-19, Fraunhofer found particles up to 3.205µm. In both Mie analysis no larger particles than 452nm were detected, but were seen in images from microscopy. The results indicate that a correct index of refraction is not the only important parameter for a correct analysis.

The stearyl aclcohol NLCs without tretinoine (Table 5-20) contained large particles, as detected from all LD measurements. In this case the analysis by microscopy did not show any larger particles. From this it is shown again, that also microscopy can lead to errors of analysis.

The analysis of NLCs containing tretinoine (Table 5-21) detected no particles larger 3.5µm within LD analysis. Also microscopy showed only a single crystal of 30µm.

Table 5-13: Data of Lipofundin MCT 10%
Comparison of PCS diameter (z-average) and LD diameters calculated with Fraunhofer (blue) and Mie using the standard values after (Müller 1996) (orange) and the measured RI and IRI (green) (upper right), the corresponding LD distribution curves (middle), the corresponding microscopic picture (upper left), the full simulation of the LD raw data (using optical parameters ranging from 1.3-1.8 for RI and from 0-1 for IRI) (lower), LD measurement was performed with included PIDS

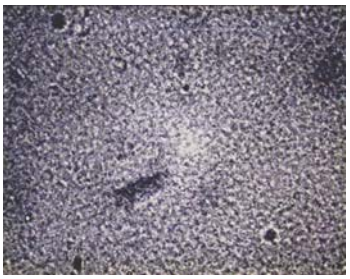

5µm
magnification: 1000x

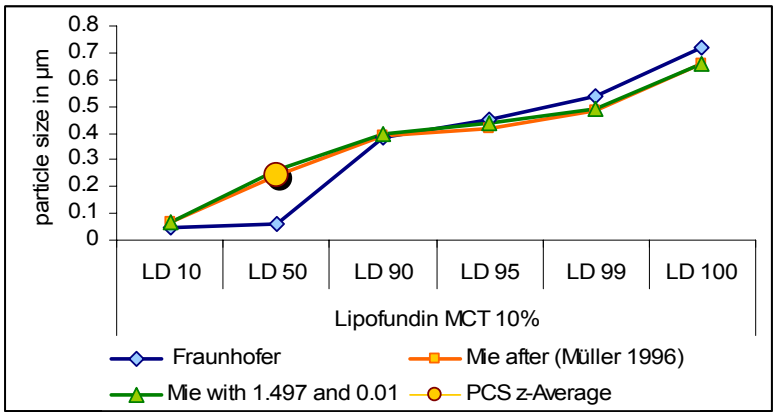

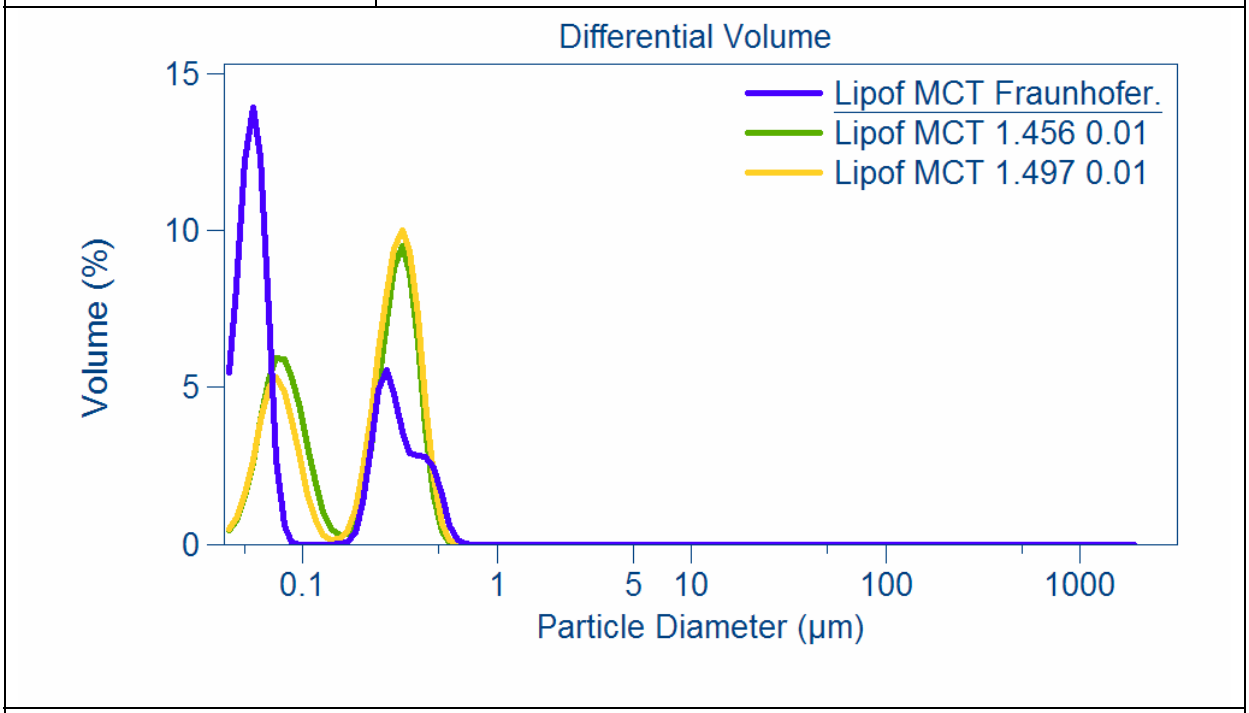

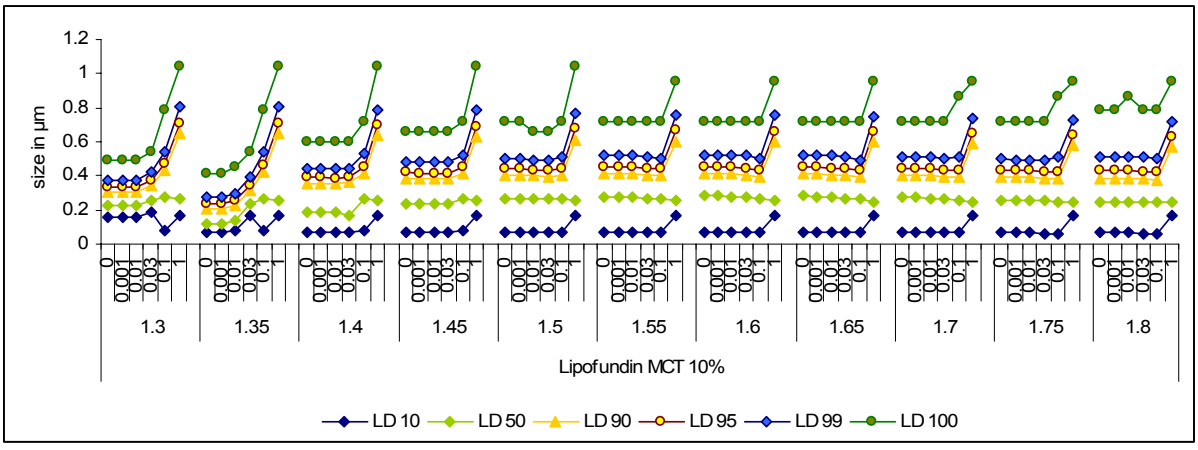

Table 5-14: Data of Lipofundin N 10%
Comparison of PCS diameter (z-average) and LD diameters calculated with Fraunhofer (blue) and Mie using the standard values after (Müller 1996) (orange) and the measured RI and IRI (green) (upper right), the corresponding LD distribution curves (middle), the corresponding microscopic picture (upper left), the full simulation of the LD raw data (using optical parameters ranging from 1.3-1.8 for RI and from 0-1 for IRI) (lower), LD measurement was performed with included PIDS

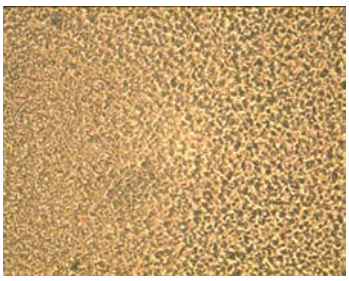

5µm
magnification: 1000x

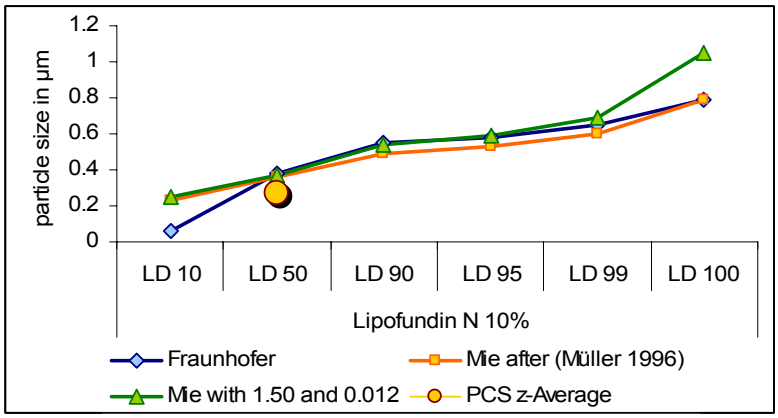

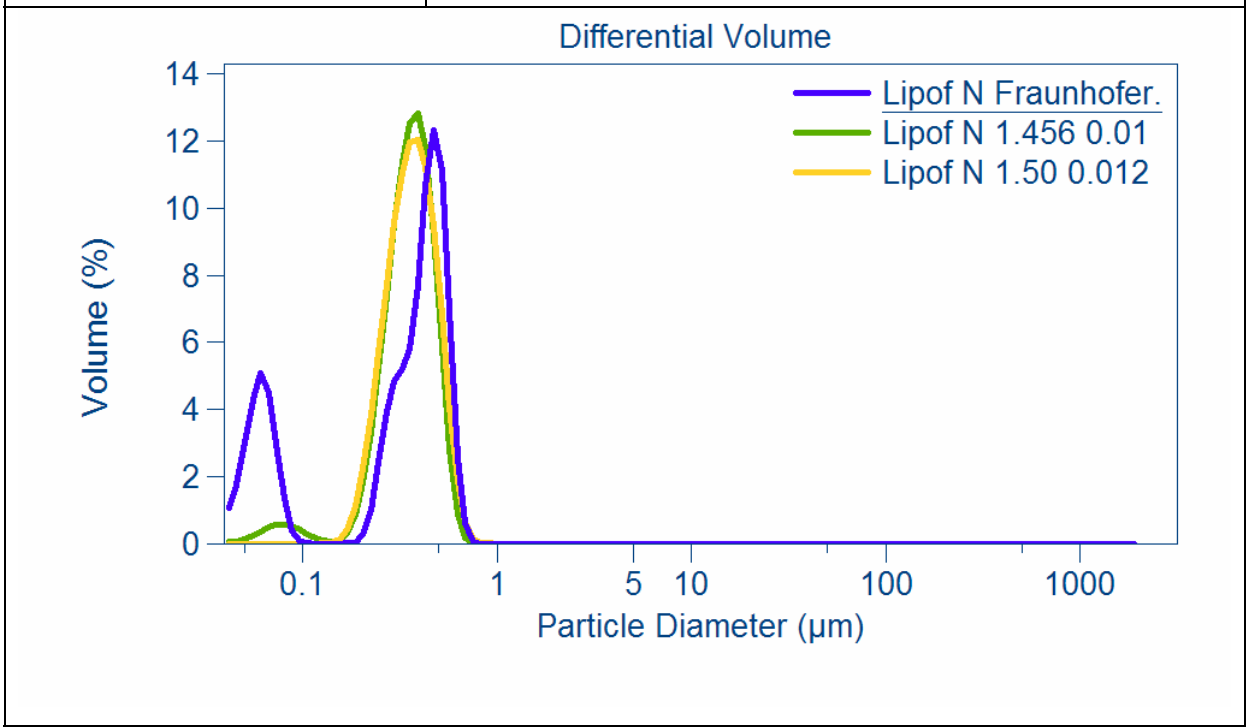

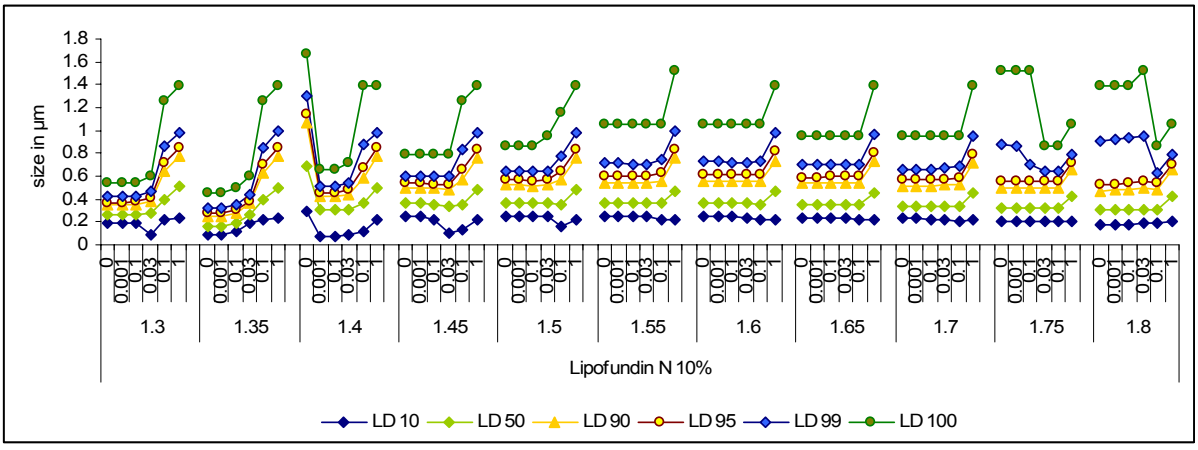

Table 5-15: Data of Stab 1 (lipid phase: cetylpalmitate and Miglyol 812, stabiliser: Tegocare 450) Comparison of PCS diameter (z-average) and LD diameters calculated with Fraunhofer (blue) and Mie using the standard values after (Müller 1996) (orange) and the measured RI and IRI (green) (upper right), the corresponding LD distribution curves (middle), the corresponding microscopic picture (upper left), the full simulation of the LD raw data (using optical parameters ranging from 1.3-1.8 for RI and from 0-1 for IRI) (lower), LD measurement was performed with included PIDS

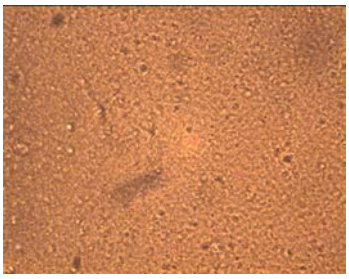

5µm
magnification: 1000x

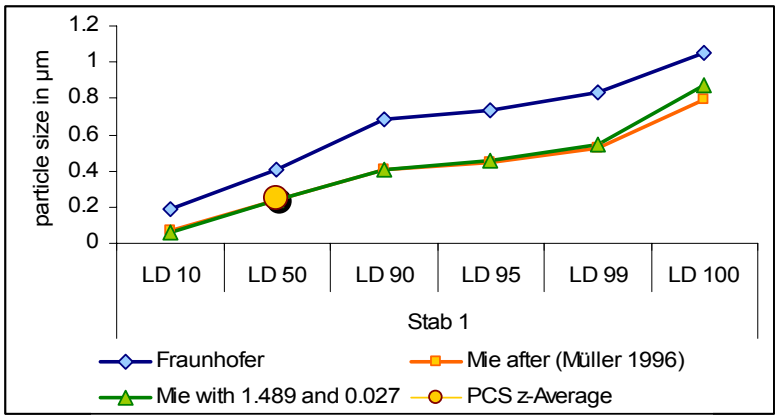

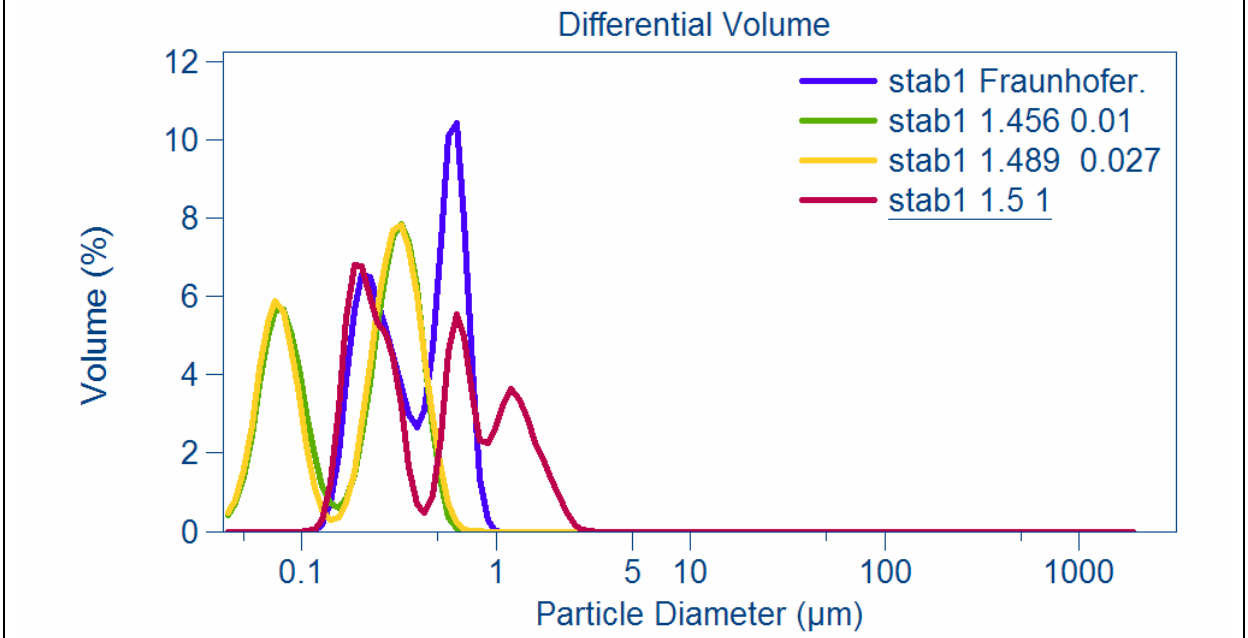

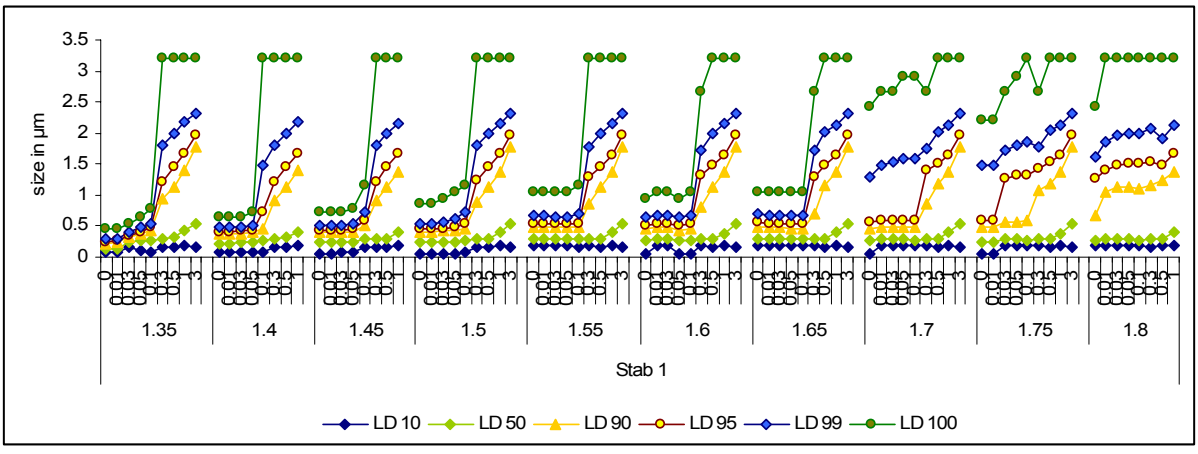

Table 5-16: Data of Stab 2 (lipid phase: cetylpalmitate and Miglyol 812, stabiliser: Poloxamer 188) Comparison of PCS diameter (z-average) and LD diameters calculated with Fraunhofer (blue) and Mie using the standard values after (Müller 1996) (orange) and the measured RI and IRI (green) (upper right), the corresponding LD distribution curves (middle), the corresponding microscopic picture (upper left), the full simulation of the LD raw data (using optical parameters ranging from 1.3-1.8 for RI and from 0-1 for IRI) (lower), LD measurement was performed with included PIDS

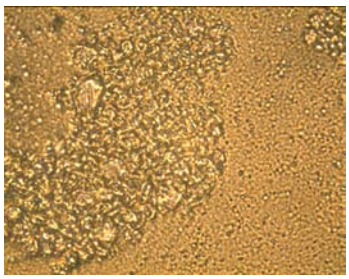

5µm
magnification: 1000x

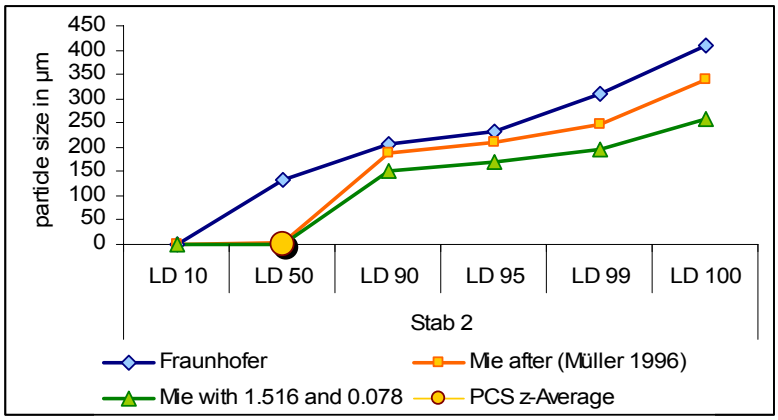

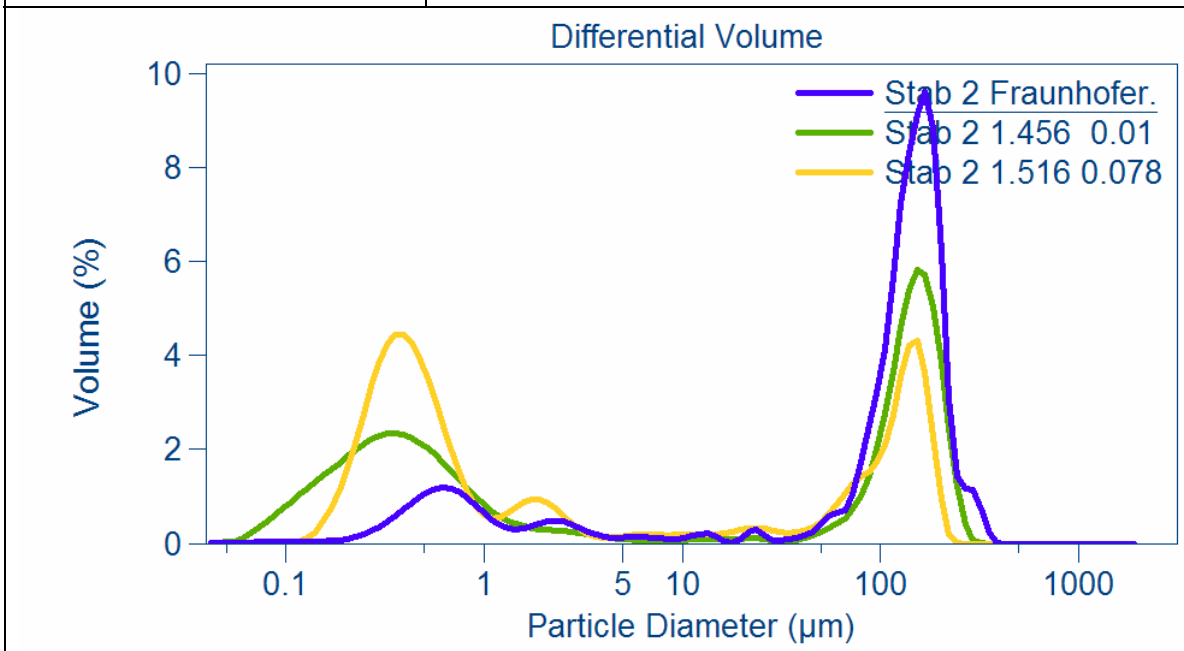

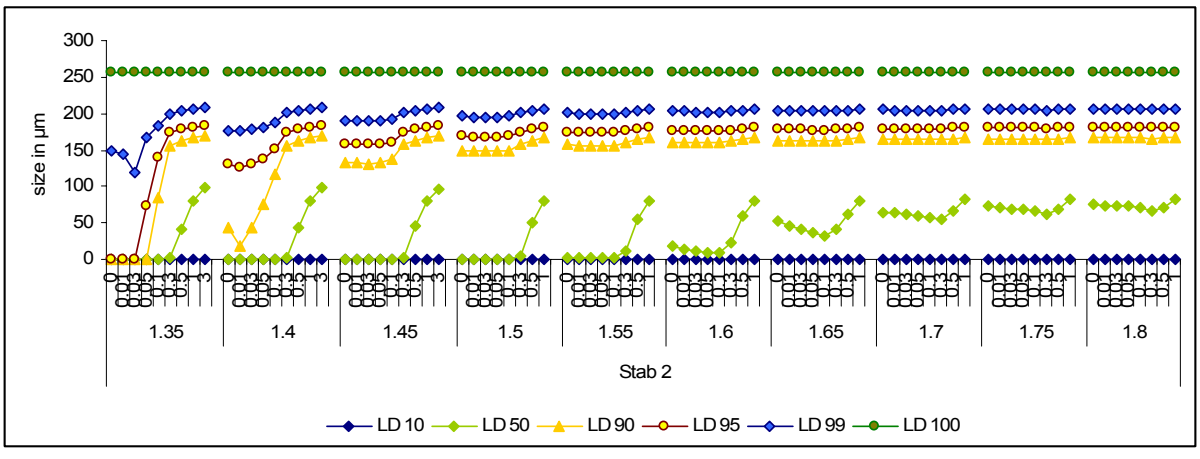

Table 5-17: Data of Stab 3(lipid phase: cetylpalmitate and Miglyol 812, stabiliser: Tween 80) Comparison of PCS diameter (z-average) and LD diameters calculated with Fraunhofer (blue) and Mie using the standard values after (Müller 1996) (orange) and the measured RI and IRI (green) (upper right), the corresponding LD distribution curves (middle), the corresponding microscopic picture (upper left), the full simulation of the LD raw data (using optical parameters ranging from 1.3-1.8 for RI and from 0-1 for IRI) (lower), LD measurement was performed with included PIDS

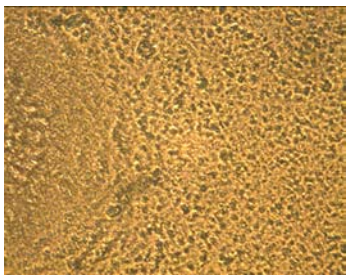

5µm
magnification: 1000x

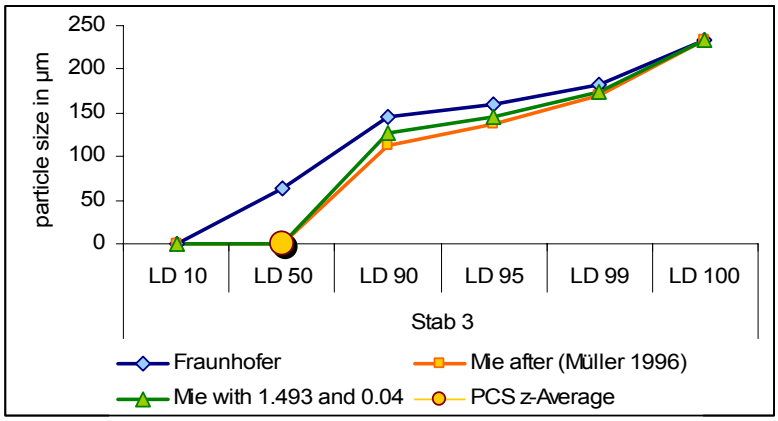

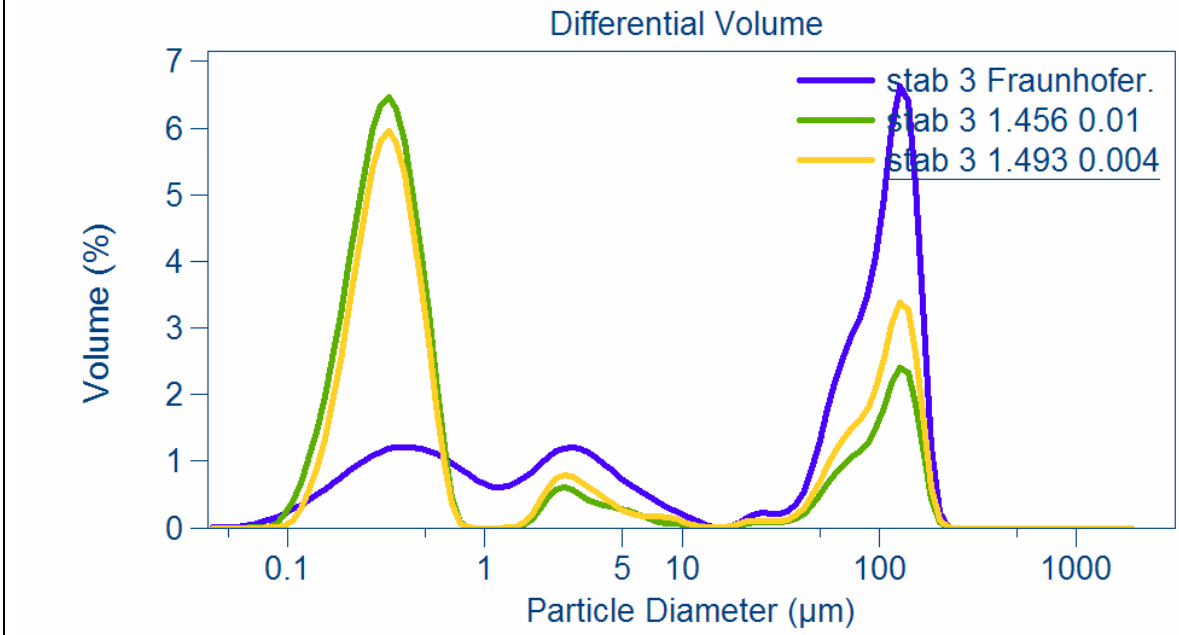

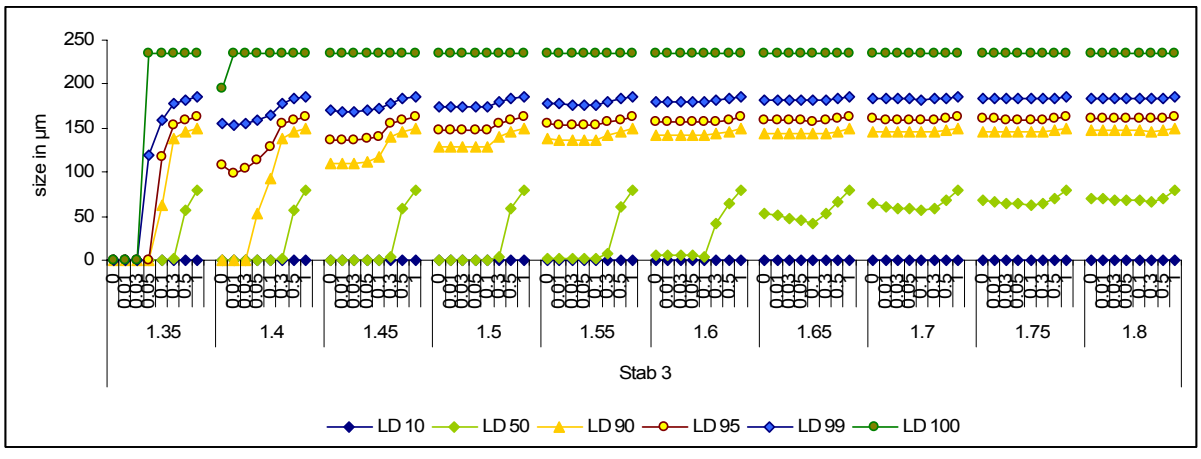

Table 5-18: Data of cetylpalimitate SLN stabilised with lecithin
Comparison of PCS diameter (z-average) and LD diameters calculated with Fraunhofer (blue) and Mie using the standard values after (Müller 1996) (orange) and the measured RI and IRI (green) (upper right), the corresponding LD distribution curves (middle), the corresponding microscopic picture (upper left), the full simulation of the LD raw data (using optical parameters ranging from 1.3-1.8 for RI and from 0-1 for IRI) (lower), LD measurement was performed with included PIDS

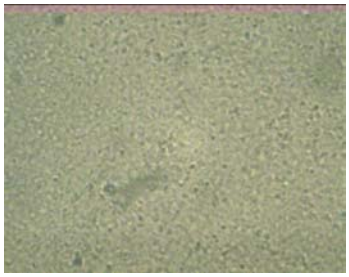

5µm
magnification: 1000x

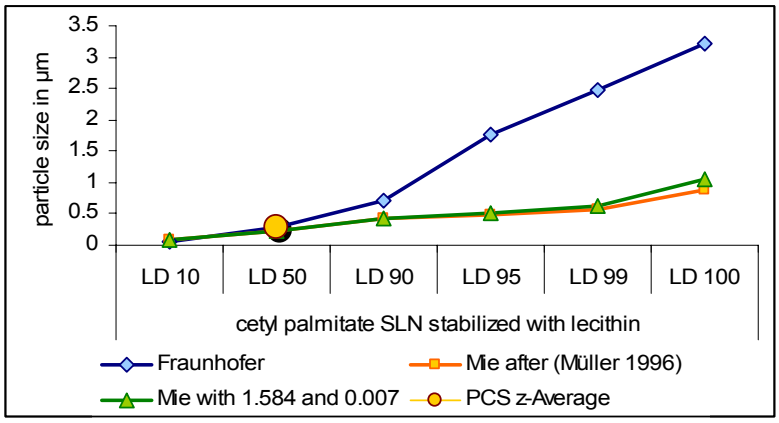

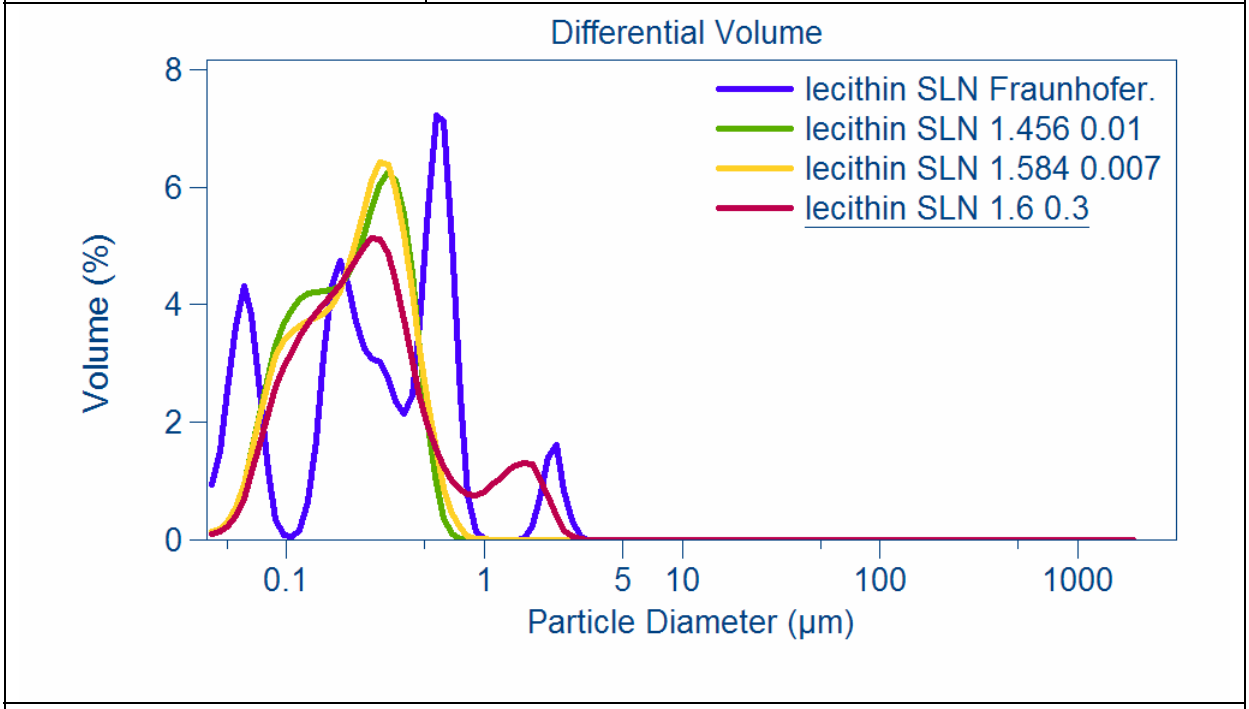

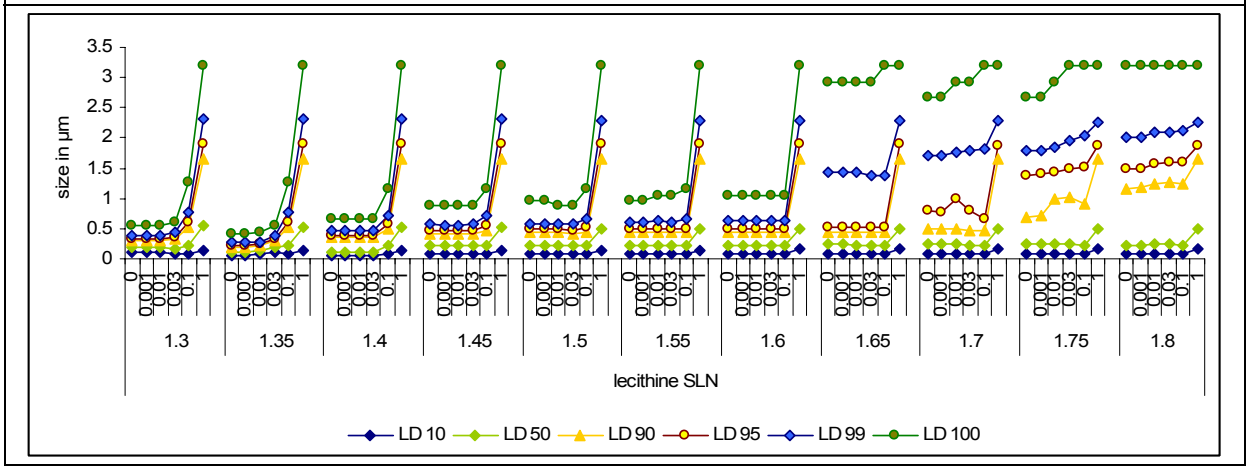

Table 5-19: Data of Dynasan NLC
Comparison of PCS diameter (z-average) and LD diameters calculated with Fraunhofer (blue) and Mie using the standard values after (Müller 1996) (orange) and the measured RI and IRI (green) (upper right), the corresponding LD distribution curves (middle), the corresponding microscopic picture (upper left), the full simulation of the LD raw data (using optical parameters ranging from 1.3-1.8 for RI and from 0-1 for IRI) (lower), LD measurement was performed with included PIDS

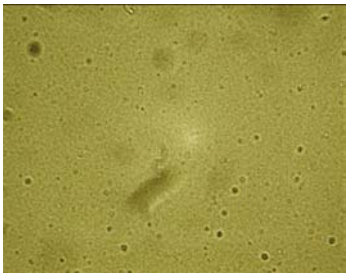

5µm
magnification: 1000x

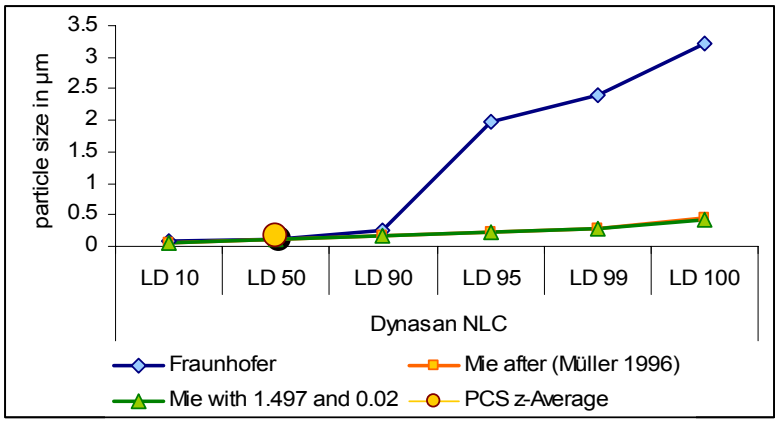

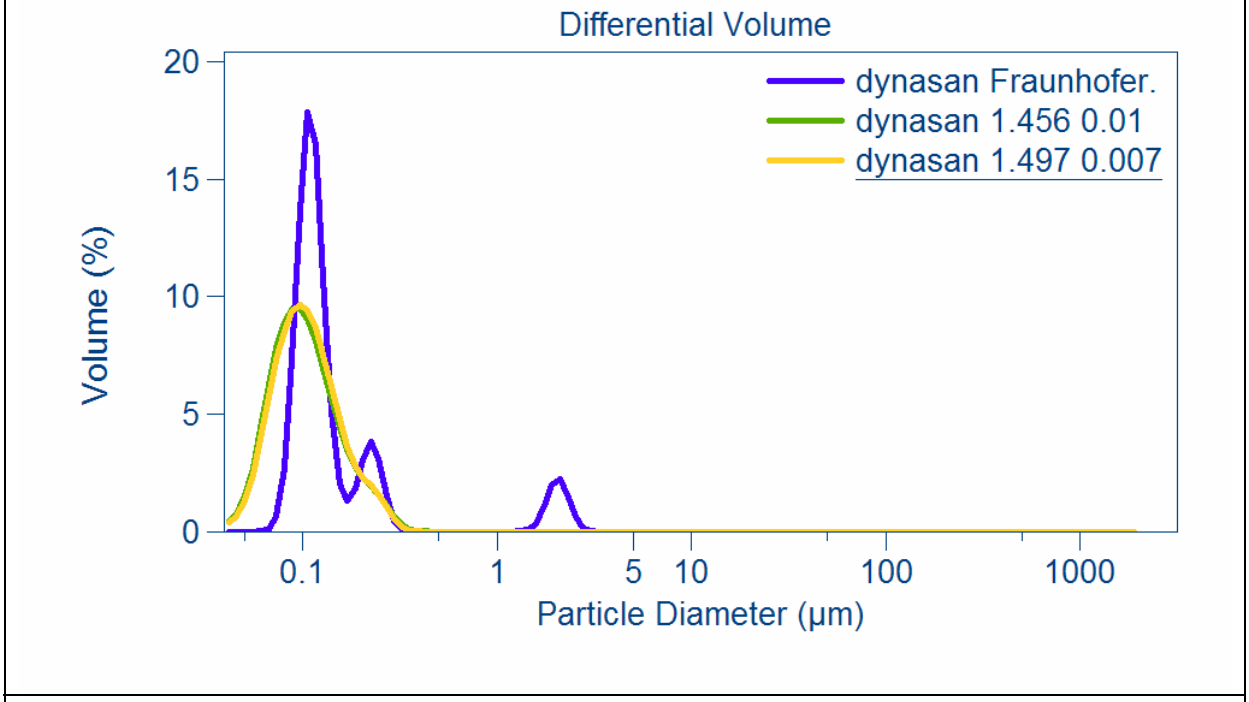

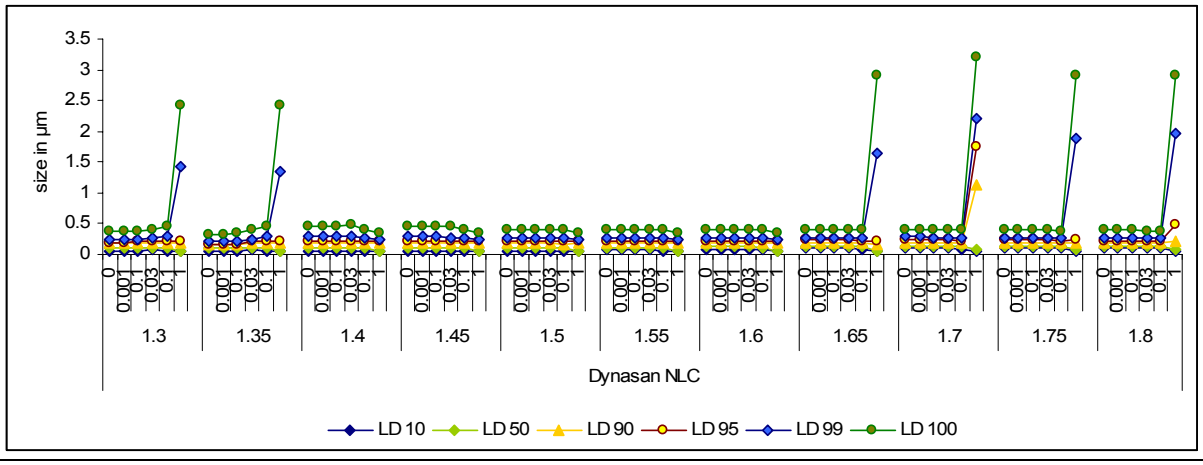

Table 5-20: Data of stearyl alcohol NLC without tretinoine
Comparison of PCS diameter (z-average) and LD diameters calculated with Fraunhofer (blue) and Mie using the standard values after (Müller 1996) (orange) and the measured RI and IRI (green) (upper right), the corresponding LD distribution curves (middle), the corresponding microscopic picture (upper left), the full simulation of the LD raw data (using optical parameters ranging from 1.3-1.8 for RI and from 0-1 for IRI) (lower), LD measurement was performed with included PIDS

50µm
magnification: 160x

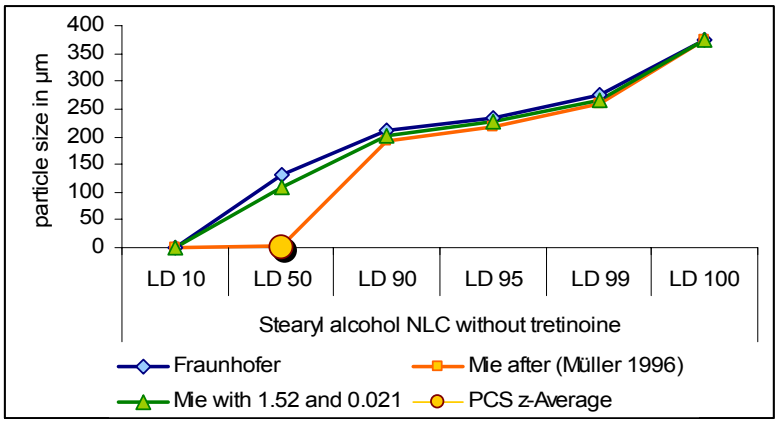

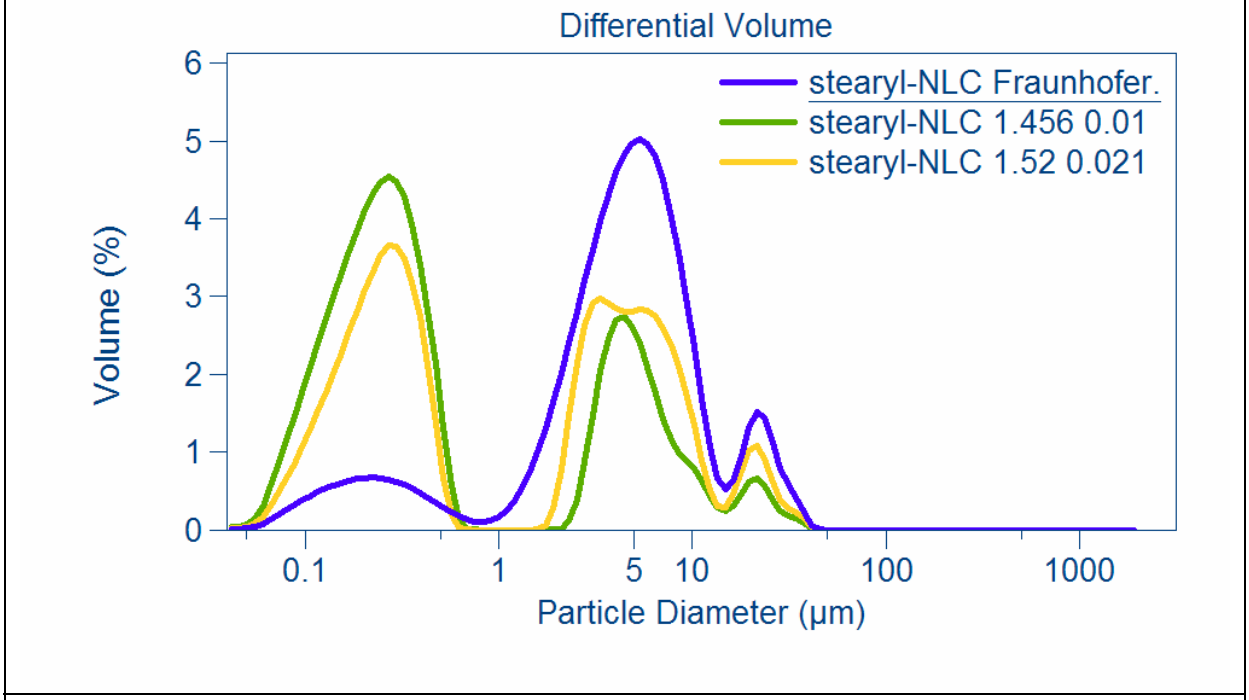

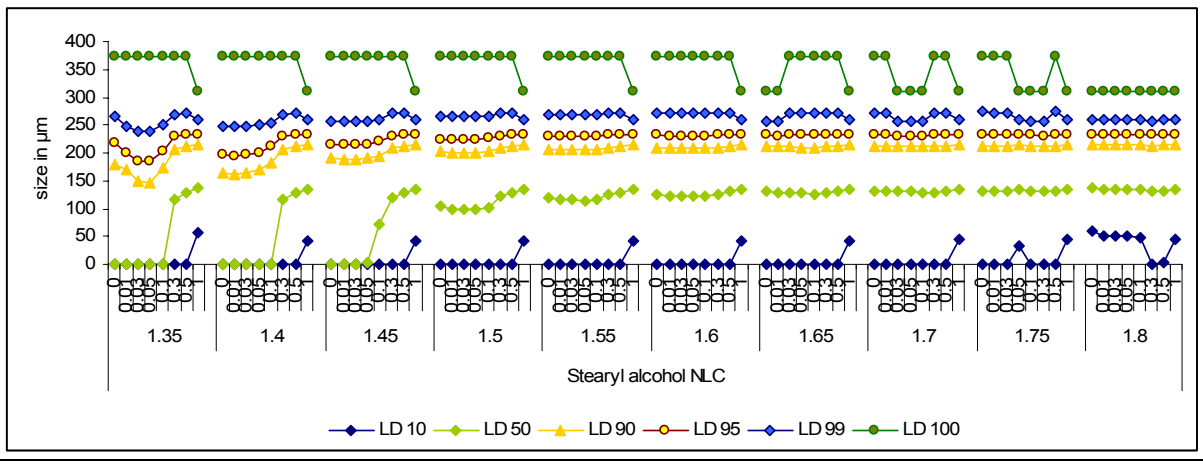

Table 5-21: Data of stearyl alcohol NLC containing the drug tretinoine
Comparison of PCS diameter (z-average) and LD diameters calculated with Fraunhofer (blue) and Mie using the standard values after (Müller 1996) (orange) and the measured RI and IRI (green) (upper right), the corresponding LD distribution curves (middle), the corresponding microscopic picture (upper left), the full simulation of the LD raw data (using optical parameters ranging from 1.3-1.8 for RI and from 0-1 for IRI) (lower), LD measurement was performed with included PIDS

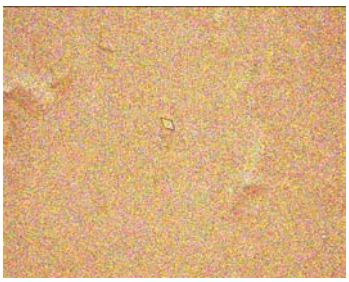

50µm
magnification: 160x

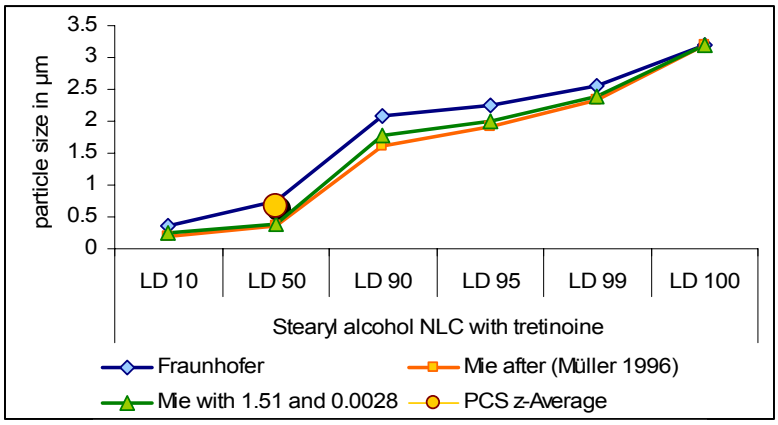

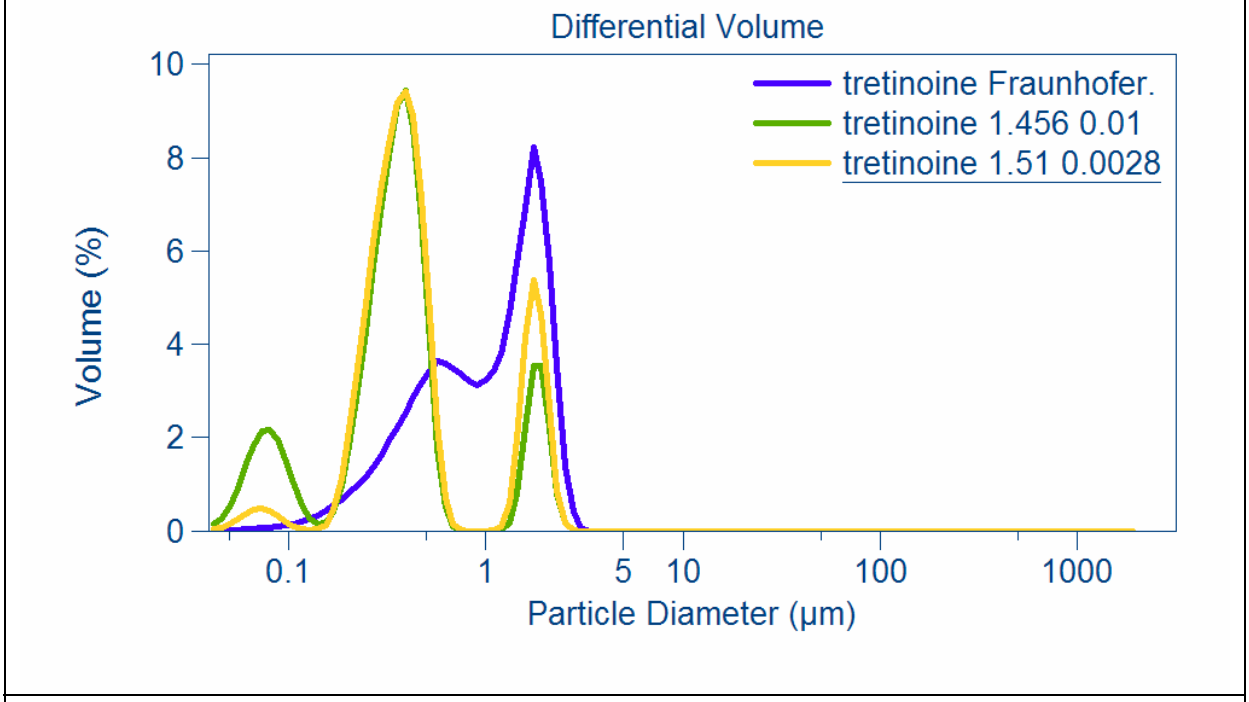

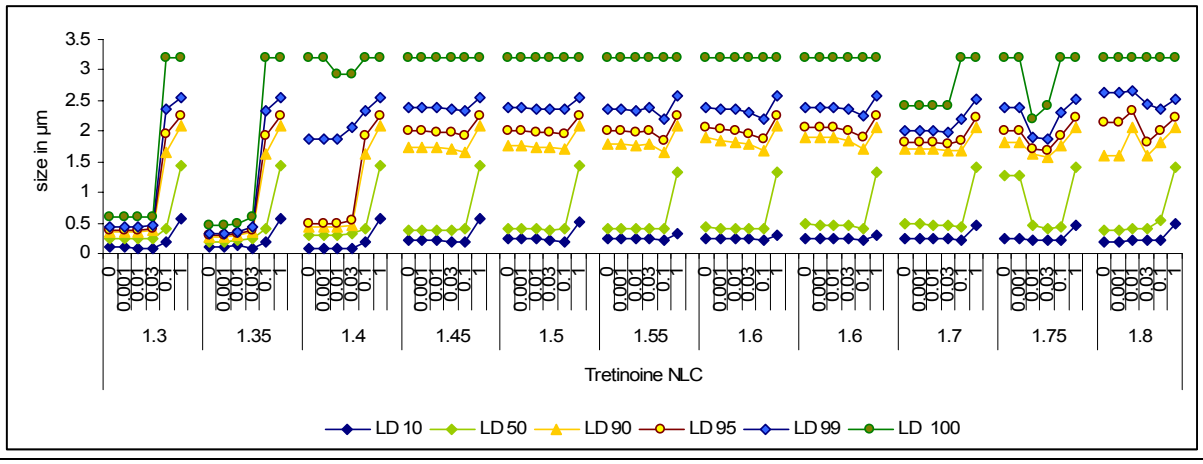

Table 5-22: Data of Azodicarbonamide nanosuspension
Comparison of PCS diameter (z-average) and LD diameters calculated with Fraunhofer (blue) and Mie using the standard values after (Müller 1996) (orange) and the measured RI and IRI (green) (upper right), the corresponding LD distribution curves (middle), the corresponding microscopic picture (upper left), the full simulation of the LD raw data (using optical parameters ranging from 1.3-1.8 for RI and from 0-1 for IRI) (lower), LD measurement was performed with included PIDS

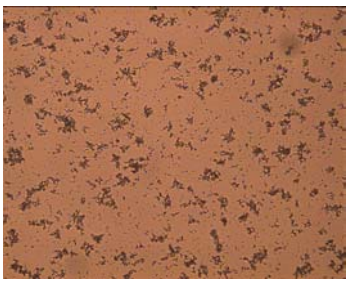

50µm
magnification: 160x

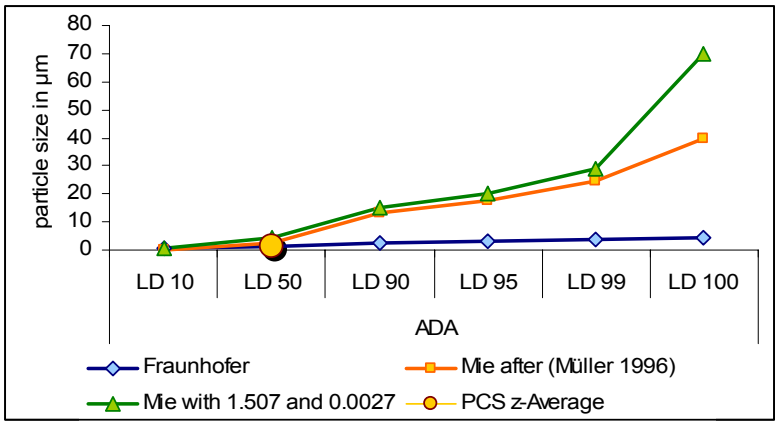

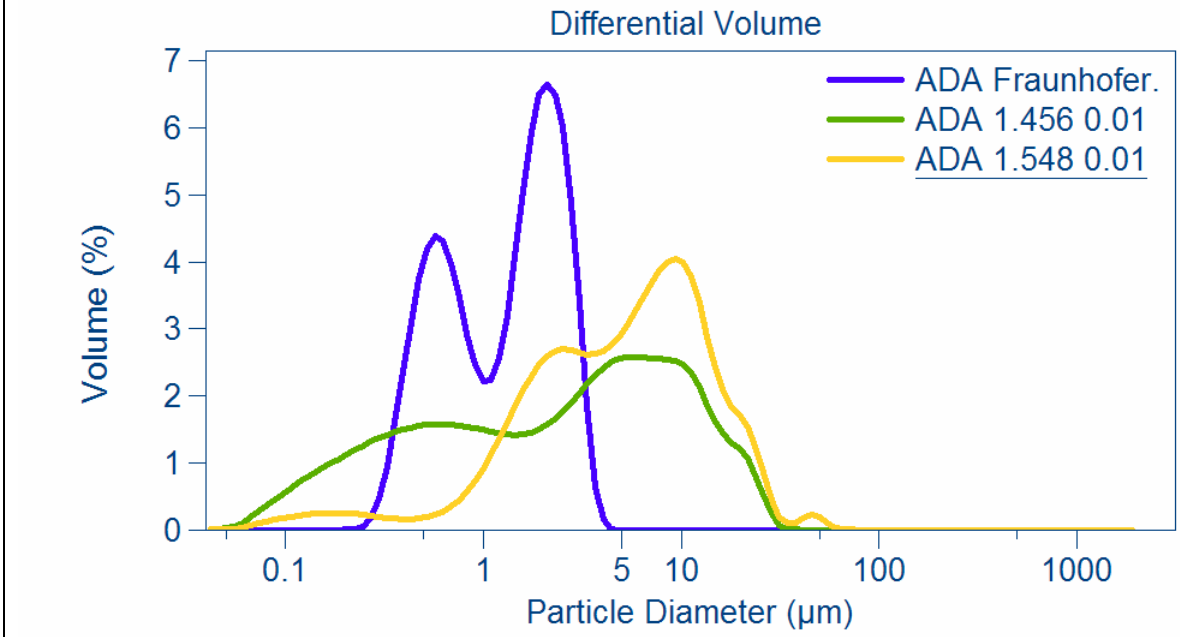

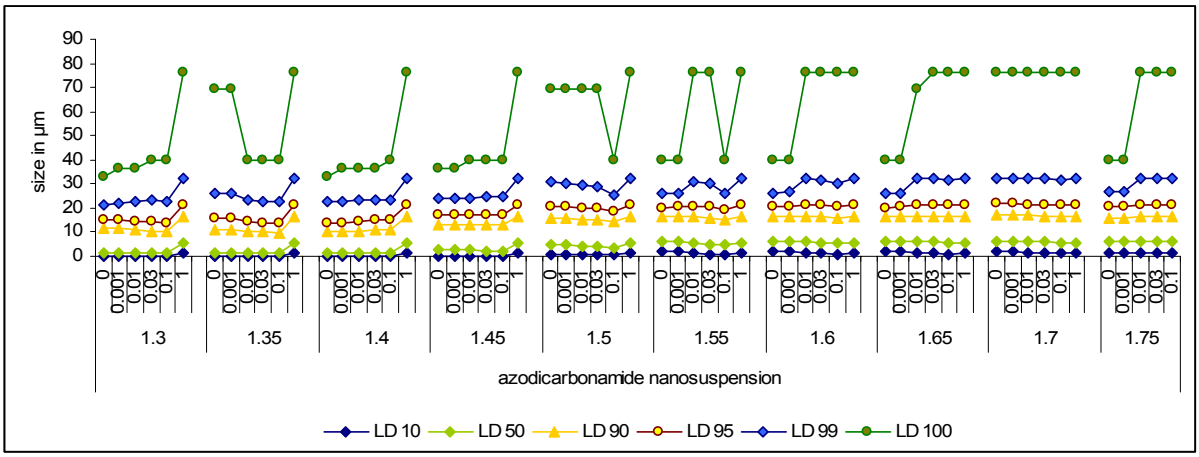

Table 5-23: Data of cyclosporine nanosuspension
Comparison of PCS diameter (z-average) and LD diameters calculated with Fraunhofer (blue) and Mie using the standard values after (Müller 1996) (orange) and the measured RI and IRI (green) (upper right), the corresponding LD distribution curves (middle), the corresponding microscopic picture (upper left), the full simulation of the LD raw data (using optical parameters ranging from 1.3-1.8 for RI and from 0-1 for IRI) (lower), LD measurement was performed with included PIDS

5µm
magnification: 1000x

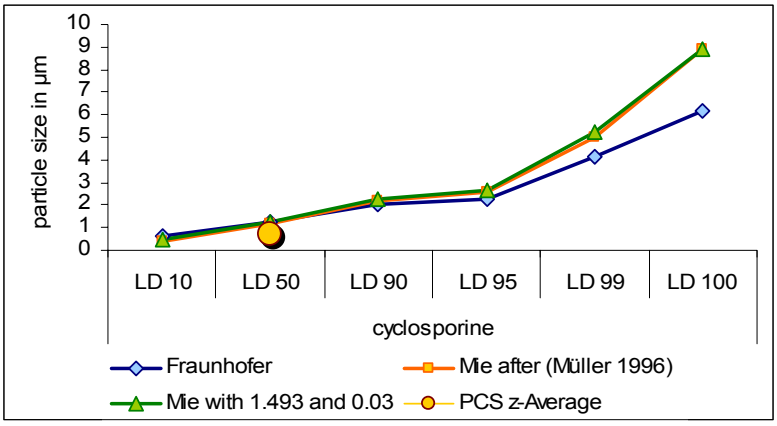

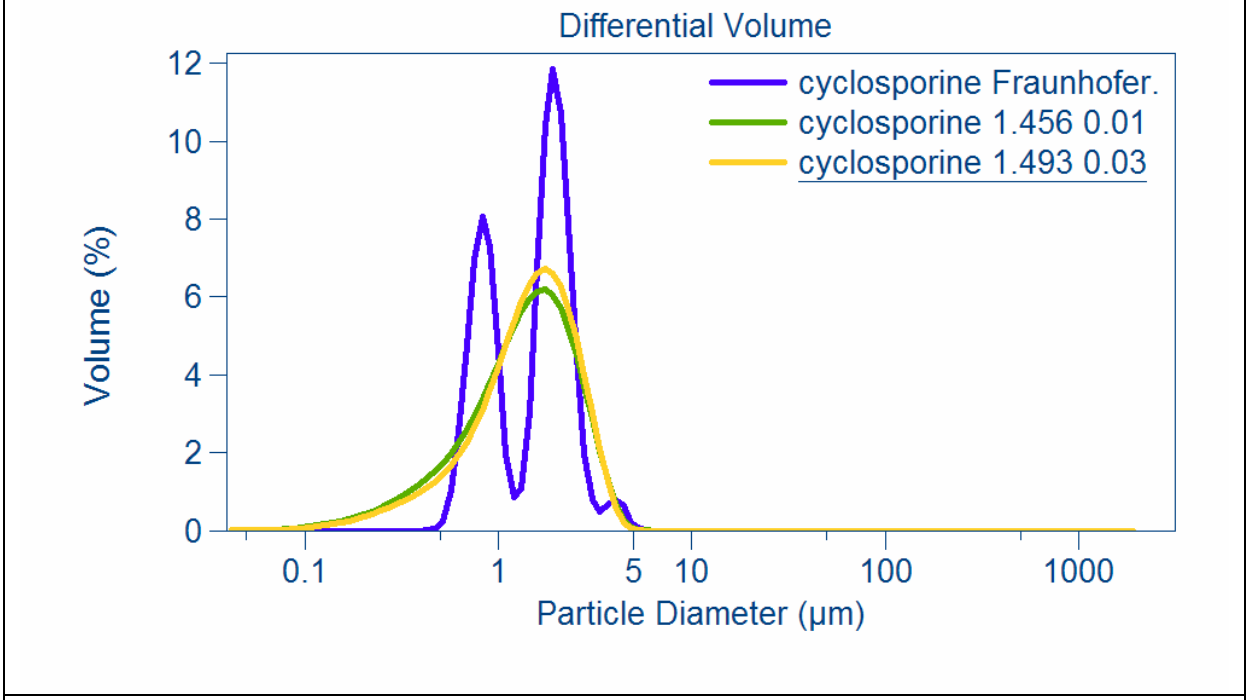

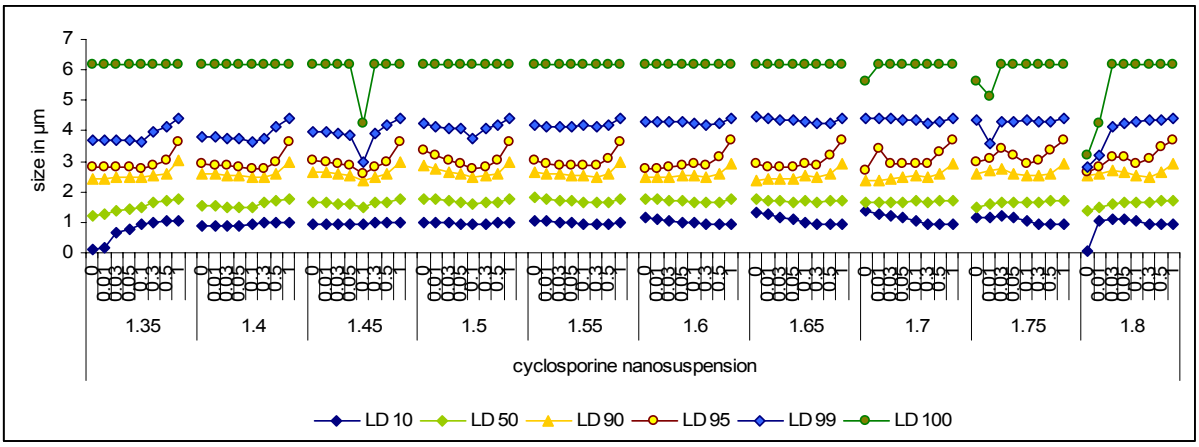

However this NLC suspension was known to be highly polydisperse. Particle size characterisation in this way leads to fatal errors, even though if the optical parameters are correct. The reason was found to be the inclusion of PIDS into the measurement, which over estimates small particles. Therefore this system as well as dynasan SLN and the cyclosporine nanosuspension were analysed again without PIDS. For all systems now larger particles were clearly detected (Figure 5-11).

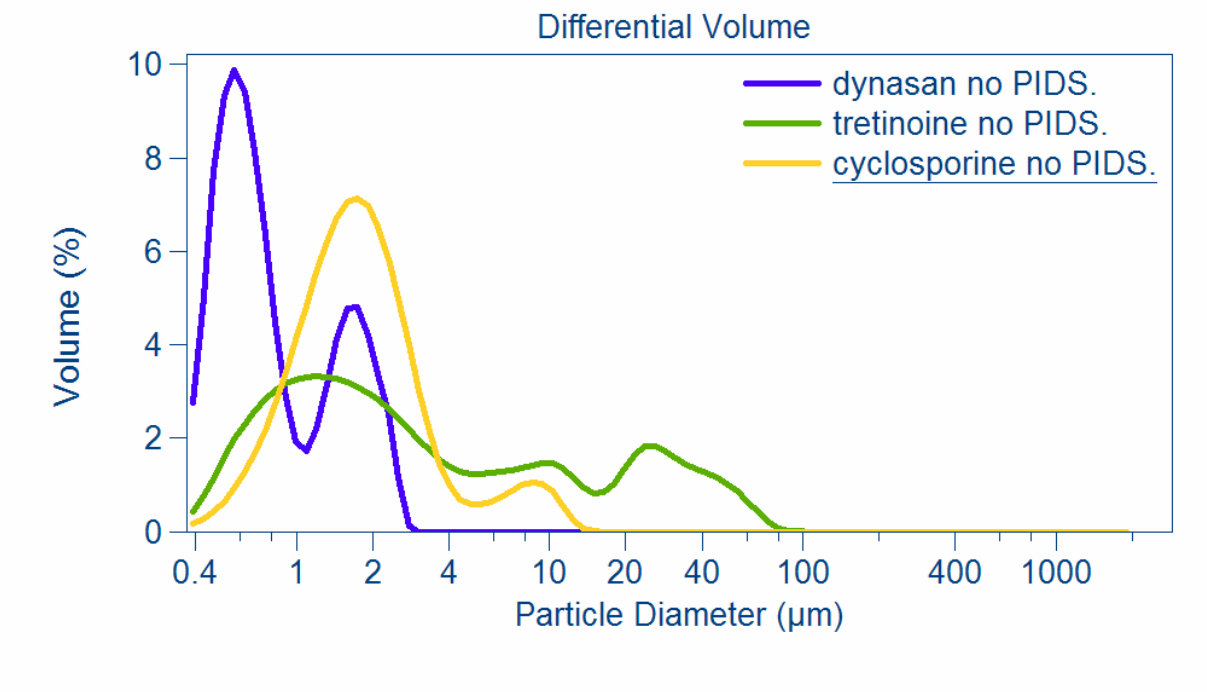

Figure 5-11: LD data without PIDS from Dynasan SLN, Tretinoine SLN and cyclosporine nanosuspension

The analysis of the nanosuspension containing azodicarbonamide by light microscopy showed a highly agglomerated system (Table 5-22). This was not detected when Fraunhofer approximation was applied. If Mie theory was applied, larger particles could be analysed. However, differences can be seen in the distribution graph. Mie theory with the standard value gives maximal particle sizes of only 40µm, whereas the maximal value was 80µm if the determined correct refractive index was used. The analysis of the cyclosporine nanosuspension (Table 5-23) shows a trimodale distribution for the system if Fraunhofer approximation is used. Mie calculations were very similar to each other and only found a monomodal distribution. In the LD chapter the performance of the LS 230 was investigated by using various mixtures of latex dispersions. None of the results was analysed correctly, when Fraunhofer approximation was applied. Therefore also the result obtained from Fraunhofer analysis for the cyclosporine nanosuspension is expected to be an artificial distribution.

5.3.1 Conclusion

The comparison of all results obtained from these measurements gave very distinct results. In some of the systems analysed, large particles were not found, either by microscopy or/and by laser diffractometry.

Fraunhofer approximation often failed to characterise the system correctly. The comparison of both Mie calculations (standard after (Müller 1996) vrs. correctly determined index) also gave different results. In most of the cases the difference between the results was only very small, whereas in some of the cases very different results were obtained. From the simulations, where various optical parameters were used it was found that every system is influenced differently by these parameters. Some systems gave stronger variations than others. This was also found for the size distribution curves. Some size distributions changed from bimodal to monomodal or trimodal. However taking into account the findings from the nailing test, those distributions are not necessarily correct or true. In conclusion the LS 230 is not the appropriate instrument for the detection of polydisperse but narrow systems in the submicron range. Therefore the interpretation of calculated polydisperse results should be done with caution. All over it is more important to measure the systems also without PIDS, as only here larger particles are detected reliably.